SHEAR STABILITY OF FLAT PANELS OF SANDWICH CONSTRUCTION

Revised May 1962

No. 1560

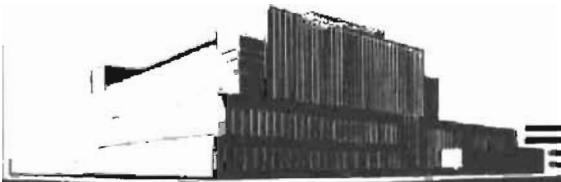

FOREST PRODUCTS LABORATORY
MADISON 5, WISCONSIN

UNITED STATES DEPARTMENT OF AGRICULTURE
FOREST SERVICE
In Cooperation with the University of Wisconsin

SHEAR STABILITY OF FLAT PANELS OF SANDWICH CONSTRUCTION[1]

By

EDWARD W. KUENZI, Engineer
W. S. ERICKSEN, Mathematician
and
JOHN J. ZAHN, Engineer

Forest Products Laboratory,[2] Forest Service
U.S. Department of Agriculture

Abstract

A theoretical analysis is presented of the behavior of sandwich panels having dissimilar facings of unequal thickness when loaded in edgewise shear. Design curves are presented for simply supported panels with dissimilar facings. Approximate formulas are included for clamped panels. The analysis is compared with results of tests on 28 square panels of symmetrical isotropic sandwich constructions. Included are descriptions of testing techniques employed to induce pure shear in the test panels. A method is given for predicting the behavior at stresses exceeding proportional-limit values.

Introduction

The purpose of this work was to obtain information concerning the elastic stability of flat panels of sandwich construction subjected to edgewise shear, and to make possible the rational design of such panels.

---

[1]This progress report is one of a series (ANC-23, Item 58-2) prepared and distributed by the Forest Products Laboratory under Bureau of Naval Weapons Order No. 19-61-8041-WEPS and U.S. Air Force Order No. DO 33(616)61-06. Results here reported are preliminary and may be revised as additional data become available. Orignial report dated May 1947.

[2]Maintained at Madison, Wis., in cooperation with the University of Wisconsin.

The work done consists of (1) a theoretical development of formulas and charts by which the critical loads can be predicted, and (2) of tests to obtain an estimate of the reliability of these predictions. A discussion of the methods used in the analysis together with a summary of results is presented. The formulas by which the critical loads are determined are developed in Appendix A.

Two types of support were considered; namely, all edges simply supported and all edges clamped. The simply supported panels are assumed to have orthotropic cores and dissimilar orthotropic facings. For all edges clamped, however, the analysis is confined to isotropic cores and facings of similar isotropic materials.

In order to apply the results of this analysis, much tedious calculation is necessary. Hence, design curves are presented that were obtained with the aid of a digital computer. In all of the computations, the bending stiffness of the individual facings were assumed to be negligible because the facings were usually very thin. Calculations were carried out for the simply supported case only. Clamped panels are analyzed, but no curves are presented. Instead, a conservative approximate design formula is given, which utilizes the known results for homogeneous isotropic panels and modifies them for isotropic sandwich constructions.

Notation

a	-- width of panel
b	-- length of panel
B_j, B_j'	-- see equations (A 34)[3] and (A 38)
c	-- core thickness
C_{mn}, C_m, D_m	-- Fourier coefficients of deflection expressions
c_i, $i = 1, \ldots, 5$	-- see equation (A 40)
D, $D_f^{(i)}$, $i = 1, 2$	-- flexural rigidities. See equations (2) and (10).

[3]When equation number is preceded by an A, this refers to an equation in Appendix A.

E_{xi}, E_{yi}, $i = 1, 2$	-- Young's moduli of orthotropic facings
E_i, $i = 1, 2$	-- Young's moduli of isotropic facings
E_f	-- Young's modulus of isotropic facings
e_{zx}, e_{yz} $e_{xx}^{(i)}$, $i = 1, 2$ etc.	-- strains. See equations (A 6) and (A 7).
f_1, f_2	-- facing thicknesses
$F_{mn}^{(1)}$, $F_{mn}^{(2)}$, $F_{mn}^{(12)}$	-- see equation (10)
F_{mn}	-- see equation (13)
h	-- $c + \frac{1}{2}(f_1 + f_2)$ centroidal distance between facings
H_{mn}^{rs}	-- see equation (10)
H_r^s	-- see equation (21)
K_{mn}, L_{mn} $L_{mn}^{(i)}$	-- see equations (10) and (13)
L_o	-- value of L_{cr} at $S = 0$
L_{cr}, L_{xy}	-- buckling coefficients. See equation (1).
N_{cr}, N_{xy}	-- loading in force per unit length of edge.
S_x, S_y, S	-- core shear parameters. See equation (4). No subscript used when core is isotropic.

S_{xl}, S_l -- limiting value of core shear parameter beyond which buckling is associated with core shear instability. See equations (6), (7), and (8).

t -- dimensionless parameter indicating relative membrane stiffness of dissimilar facings. See equation (10).

T_i, $i = 1, 2$ -- facing membrane stiffness. See equation (10).

U, U_L -- see equations (A 8) and (A 10)

$V_{mn}^{(i)}$, $i = 1, 2$; V_{mn} -- see equation (10)

w -- deflection of panel in z direction

x, y, z -- coordinate axes. See figure 1.

α_i, β_i, γ_i, $i = 1, 2$ -- dimensionless facing properties. See equation (10).

δ -- halfwave length of a buckle in an infinitely long panel. See equation (A 24).

σ_{xyi}, σ_{yxi}, $i = 1, 2$ -- Poisson's ratios of facings.

$\lambda_i = 1 - \sigma_{xyi}\,\sigma_{yxi}$

μ'_{zx}, μ'_{yz} -- moduli of rigidity of core

$$\theta = \frac{S_y}{S_x} = \frac{\mu'_{zx}}{\mu'_{yz}}$$

η -- slope of deflection nodal lines. See equations (A 32) and (A 33).

ψ_{mn} -- see equation (10).

Results and Discussion

Buckling Load Factor

The buckling load factor is defined as

$$L_{cr} = \frac{N_{cr} \; a^2}{\pi^2 \; D} \tag{1}$$

where

$$\left.\begin{aligned} D &= \frac{T_1 \, T_2 \, h^2}{T_1 + T_2} \\ T_i &= \frac{\sqrt{E_{xi} \, E_{yi}} \; f_i}{\lambda_i} \;, \quad i = 1, \; 2 \\ \lambda_i &= 1 - \sigma_{xyi} \, \sigma_{yxi} \;, \quad i = 1, \; 2 \\ h &= c + \frac{f_1 + f_2}{2} \end{aligned}\right\} \tag{2}$$

Here h is the centroidal distance between facings, T is the membrane stiffness of a facing, σ_{xy} and σ_{yx} are the Poisson's ratios of a facing, D is the bending stiffness of the panel, and N_{cr} is the critical load in pounds per inch of edge.

L_{cr} depends upon the aspect ratio $\frac{a}{b}$, the relative membrane stiffness

$$t = \frac{T_1}{T_1 + T_2} \tag{3}$$

and two core shear parameters

$$\left.\begin{aligned} S_x &= \frac{c}{h^2 \mu'_{zx}} \cdot D \frac{\pi^2}{a^2} \\ \text{and} \qquad S_y &= \theta S_x \;, \quad \theta = \frac{\mu'_{zx}}{\mu'_{yz}} \end{aligned}\right\} \tag{4}$$

which account for the effect of the transverse shear deformations in the core. When $S_x = 0$ and the facings are isotropic, the theory reduces to that for a homogeneous isotropic plate with stiffness equal to $\underline{D}$ given above.

Buckling by Core Shear Instability

As S_x increases, the effect of the transverse shear deformation increases and the theoretical buckling load decreases, with a larger number of buckles.

The limiting behavior of the panel when S_x is large is treated separately, and it is found that for sufficiently large S_x the buckling load factor depends only on the core shear parameters and is given by

$$L_{cr} = \frac{1}{\sqrt{S_x S_y}} \tag{5}$$

for $S_x \geq S_{x1}$ where S_{x1} depends upon θ, $\frac{a}{b}$, t, and facing properties. Explicit formulas for S_{x1} have been worked out for the case of simply supported panels with similar isotropic facings in which case

$$S_{x1} = \frac{\left(\frac{1-\sigma_f}{2}\right) 4\theta + (1-\theta)^2}{\left(\frac{1-\sigma_f}{2}\right)(1+\theta)^2 \left[\theta + \frac{a^2}{b^2}\right]} \tag{6}$$

σ_f = Poisson's ratio of facings

which reduces, for isotropic cores ($\theta = 1$), to

$$S_1 = \frac{1}{1 + \frac{a^2}{b^2}} \cdot \text{(Here } S_x = S_y = S\text{)} \tag{7}$$

For clamped panels with similar isotropic facings and isotropic cores

$$S_1 = \frac{\frac{3}{4}}{1 + \frac{a^2}{b^2}} \tag{8}$$

Note that whenever $L_{cr} = \frac{1}{\sqrt{S_x S_y}}$, $N_{cr} = \frac{h^2}{c}\sqrt{\mu'_{zx}\ \mu'_{yz}} \approx h\sqrt{\mu'_{zx}\ \mu'_{yz}}$.

This limiting behavior was analyzed under the assumption that the facings act as membranes, and yields results that are increasingly conservative as the facings are made thicker. Theoretically, for $S_x > S_{x1}$ the number of buckles is infinite, but in practice it will be finite and very large, since the facings are not actually membranes. Since S_{x1} is quite large, it is improbable that any practical sandwich construction would have such a thick, soft core as is necessary to produce this type of instability. Accordingly, the range of S_x in the design curves does not extend to S_{x1} . Buckling that is due to core shear instability is an interesting phenomenon theoretically, but is not of great practical significance. It does, however, indicate the assymptotic behavior of L_{cr} as S_x increases.

Theoretical Analysis

For both types of support that were considered, the case $\frac{a}{b} = 0$, or an infinitely long panel, was analyzed separately. The results of the analysis will be discussed in the following order:

(1) Finite, simply supported

(2) Infinite, simply supported

(3) Clamped, finite or infinite (approximate analysis)

Finite Panel, Simply Supported, $0 \leq S_x < S_{x1}$

L_{cr} is the lowest root of the determinant of the following system of equations:

$$\left(\frac{V_{mn}^{(1)} + V_{mn}^{(2)} + V_{mn}}{\frac{a}{b} L_{xy}}\right) C_{mn} + \sum_{r=1} \sum_{s=1} H_{mn}^{rs} C_{rs} = 0, \quad m, n, = 1, 2, \ldots \tag{9}$$

where

$$H_{mn}^{rs} = \begin{cases} \dfrac{32\, m\, n\, r\, s}{\pi^2 (m^2 - r^2)(n^2 - s^2)}, & \text{if } m + r \text{ and } n + s \text{ are odd} \\ 0, & \text{otherwise} \end{cases}$$

$$V_{mn}^{(i)} = \frac{D_f^{(i)}}{D} K_{mn}, \qquad i = 1, 2$$

$$D_f^{(i)} = \frac{1}{12} f_i^2 T_i, \qquad i = 1, 2$$

$$V_{mn} = \frac{t\, F_{mn}^{(1)} K_{mn}^{(2)} + (1-t) F_{mn}^{(2)} K_{mn}^{(1)} + \left(\frac{n^2 a^2}{b^2} S_x + m^2 S_y\right) F_{mn}^{(1)} F_{mn}^{(2)}}{\psi_{mn} + (t\, F_{mn}^{(1)} L_{mn}^{(2)} + (1-t) F_{mn}^{(2)} L_{mn}^{(1)}) S_x + S_x S_y F_{mn}^{(1)} F_{mn}^{(2)}}$$

$$\psi_{mn} = t^2 F_{mn}^{(1)} + 2t(1-t) F_{mn}^{(12)} + (1-t)^2 F_{mn}^{(2)}$$

$$\left.\begin{aligned} L_{mn}^{(i)} &= \alpha_i m^2 + \gamma_i \frac{n^2 a^2}{b^2} + \theta\left(\frac{1}{\alpha_i} \frac{n^2 a^2}{b^2} + \gamma_i m^2\right) \\ F_{mn}^{(i)} &= (1 - \beta_i^2) \frac{m^2 n^2 a^2}{b^2} + \gamma_i K_{mn}^{(i)} \\ K_{mn}^{(i)} &= \alpha_i m^4 + 2\beta_i \frac{m^2 n^2 a^2}{b^2} + \frac{1}{\alpha_i} \frac{n^4 a^4}{b^4} \end{aligned}\right\} i = 1, 2$$

$$F_{mn}^{(12)} = \left[\frac{1}{2}\left(\frac{\alpha_1}{\alpha_2} + \frac{\alpha_2}{\alpha_1}\right) - \beta_1 \beta_2\right] \frac{m^2 n^2 a^2}{b^2} + \frac{1}{2}(\gamma_1 K_{mn}^{(2)} + \gamma_2 K_{mn}^{(1)})$$

$$t = \frac{T_1}{T_1 + T_2}, \qquad T_i = \frac{\sqrt{E_{xi} E_{yi}}\, f_i}{\lambda_i}, \quad i = 1, 2 \tag{10}$$

$$\left.\begin{aligned}
\alpha_i &= \sqrt{\frac{E_{xi}}{E_{yi}}} \\
\beta_i &= \frac{\lambda_i}{\sqrt{E_{xi}\,E_{yi}}}\left\{\frac{E_{xi}\,\sigma_{yxi}}{\lambda_i} + 2\mu_{xyi}\right\} \\
\gamma_i &= \frac{\lambda_i\,\mu_{xyi}}{\sqrt{E_{xi}\,E_{yi}}}
\end{aligned}\right\} i = 1,\ 2 \qquad (10)$$

The $V_{mn}^{(i)}$ represent the effect of the bending stiffness of the individual facings and are usually neglected.

Reduction to Similar Facings. --If the facings are similar,

$$\left.\begin{aligned}
F_{mn}^{(1)} &= F_{mn}^{(12)} = F_{mn}^{(2)} = \psi_{mn} \equiv F_{mn} \\
K_{mn}^{(1)} &= K_{mn}^{(2)} \equiv K_{mn} \\
L_{mn}^{(1)} &= L_{mn}^{(2)} \equiv L_{mn}
\end{aligned}\right\} \qquad (11)$$

so that

$$V_{mn} = \frac{K_{mn} + \left(\frac{n^2a^2}{b^2}\,S_x + m^2 S_y\right) F_{mn}}{1 + L_{mn}\,S_x + S_x\,S_y\,F_{mn}} \qquad (12)$$

where

$$\left.\begin{aligned}
F_{mn} &= 1 - \beta^2 + \gamma\,K_{mn} \\
K_{mn} &= \alpha\,m^4 + 2\beta\,\frac{m^2n^2a^2}{b^2} + \frac{1}{\alpha}\,\frac{n^4a^4}{b^4} \\
L_{mn} &= \alpha m^2 + \gamma\frac{n^2a^2}{b^2} + \theta\left(\frac{1}{\alpha}\,\frac{n^2a^2}{b^2} + \gamma_m{}^2\right)
\end{aligned}\right\} \qquad (13)$$

Note that this reduction can also be accomplished by setting $t = 0$ in which case both facings have the properties of facing 1, or by setting $t = 1$ in which case both facings have the properties of facing 2.

Reduction to Isotropic Facings. --If both facings are isotropic,

$$\alpha_1 = \alpha_2 = \beta_1 = \beta_2 = 1, \quad \gamma_1 = \frac{1-\sigma_1}{2}, \quad \gamma_2 = \frac{1-\sigma_2}{2} \tag{14}$$

so that the only essential dissimilarity of the facings is due to Poisson's ratio. Since the influence of Poisson's ratio on the theoretical buckling load is very small, one might as well assume $\sigma_1 = \sigma_2$ and compute $\underline{V_{mn}}$ as if the facings were similar and isotropic. The important dissimilarity of the facings is due to Young's modulus, and this effect is accounted for in $\underline{D}$. This permits using the same set of curves for both similar and dissimilar isotropic facings, if $\underline{V_{mn}^{(1)}}$ and $\underline{V_{mn}^{(2)}}$ are neglected.

For dissimilar isotropic facings,

$$D = \frac{T_1 T_2 h^2}{T_1 + T_2}, \quad T_i = \frac{E_i f_i}{1-\sigma_i^2}, \quad i = 1, 2 \tag{15}$$

while for similar isotropic facings,

$$D = \frac{E_f}{(1-\sigma_f^2)} \frac{f_1 f_2 h^2}{(f_1 + f_2)} \tag{16}$$

and for both similar and dissimilar isotropic facings

$$\left.\begin{aligned}
K_{mn}^{(1)} &= K_{mn}^{(2)} = \left(m^2 + \frac{n^2 a^2}{b^2}\right)^2 \\
L_{mn}^{(1)} &= L_{mn}^{(2)} = m^2 + \left(\frac{1-\sigma_f}{2}\right) \frac{n^2 a^2}{b^2} + \theta \left[\frac{n^2 a^2}{b^2} + \left(\frac{1-\sigma_f}{2}\right) m^2\right] \\
\psi_{mn} &= F_{mn}^{(1)} = F_{mn}^{(12)} = F_{mn}^{(2)} = \frac{1-\sigma_f}{2} \left(m^2 + \frac{n^2 a^2}{b^2}\right)^2
\end{aligned}\right\} \tag{17}$$

so that

$$V_{mn} = \frac{\left[1 + \left(\frac{n^2a^2}{b^2} S_x + m^2 S_y\right)\left(\frac{1-\sigma_f}{2}\right)\right]\left(m^2 + \frac{n^2a^2}{b^2}\right)^2}{1 + \left[m^2 + \left(\frac{1-\sigma_f}{2}\right)\frac{n^2a^2}{b^2}\right]S_x + \left[\frac{n^2a^2}{b^2} + \left(\frac{1-\sigma_f}{2}\right)m^2\right] S_y + S_x S_y \left(\frac{1-\sigma_f}{2}\right)\left(m^2 + \frac{n^2a^2}{b^2}\right)^2} \tag{18}$$

Reduction to Isotropic Core. --If the core is isotropic, $\mu'_{zx} = \mu'_{yz} \equiv \mu_c$, $S_x = S_y \equiv S$, and $\theta = 1$. No important simplification in V_{mn} is possible unless the facings are isotropic and have equal Poisson's ratios, in which case

$$V_{mn} = \frac{\left(m^2 + \frac{n^2a^2}{b^2}\right)^2}{1 + S\left(m^2 + \frac{n^2a^2}{b^2}\right)} \tag{19}$$

Infinitely Long Panel, Simply Supported, $0 \leq S_x < S_{xi}$

L_{cr} is determined as the lowest root of the following system of equations

$$C_m \frac{\frac{\delta}{a}\left(V_{mn}^{(1)} + V_{mn}^{(2)} + V_{m1}\right)}{L_{xy}^2} - \sum_{s=1} C_s \left\{ \sum_{r=1} \frac{H_s^r \; H_m^r}{\frac{\delta}{a}\left(V_{r1}^{(1)} + V_{r1}^{(2)} + V_{r1}\right)} \right\} = 0, \; m = 1, 2, \ldots \tag{20}$$

where

$$H_m^r = \begin{cases} \dfrac{8mr}{\pi\,(m^2 - r^2)}, & \text{if } m + r \text{ is odd} \\ 0, & \text{otherwise,} \end{cases} \tag{21}$$

and $V_{m1}^{(1)}$, $V_{m1}^{(2)}$, and V_{m1} are obtained from the formulas given earlier for the finite panel for $V_{mn}^{(1)}$, $V_{mn}^{(2)}$, and V_{mn} by putting $n = 1$ and replacing b by δ. $\frac{\delta}{a}$ now represents the aspect ratio of a single buckle, and its value must be chosen by trial to make L_{cr} a minimum.

Finite Panel, Simply Supported

The deflection of the buckled panel is represented by

$$w = \sum_{m=1} \sum_{n=1} C_{mn} \sin \frac{m\pi x}{a} \sin \frac{n\pi y}{b}$$

The shape and number of waves in the buckled surface is different for each different combination of values for $\frac{a}{b}$, s_x, θ, α, and so forth. Thus, the particular C_{mn}'s, which are largest and most influential in describing the buckled surface, are different for each panel and are not necessarily those for which m and n are small. (When S_x is large, the number of buckles should theoretically become infinite.) Rather than simply take a large number of terms, perhaps 50, and hope thereby to include the important terms for all panels, an attempt was made to select an optimum group of 30 terms for each panel considered. This avoided the problem of excessive cumulative round-off error, which is always a danger when working with a large order determinant.

Because the determinant of system (9) contains so many zeros it factors into two determinants, one in which m + n is even and one in which m + n is odd. The even determinant was found to yield the lower root L_{cr} everywhere except where $0.33 \approx \left(\frac{a}{b}\right)_1 < \frac{a}{b} < \left(\frac{a}{b}\right)_2 \approx 0.55$. Accordingly, the graph L_{cr} versus $\frac{a}{b}$ is cusped as shown in figure 2.

Accuracy to within 1 percent could be maintained in the range $0 \leq S_x \leq S_{x1}$ by using the best 30 terms chosen from among the first 49 terms of the even determinant (all terms for which $m + n \leq 14$) or from among the first 56 terms of the odd determinant (all terms for which $m + n \leq 15$). The process of selecting the "best" terms is described in Appendix B.

The values of L_{cr} for a square panel with $S_x = 0$ was found to be 9.35 as compared to 9.34 found by Seydel (10)[4].

Infinitely Long Panel, Simply Supported

The deflection of the buckled panel is represented by

$$w = \sum_{m=1} \left(C_m \sin \frac{\pi y}{\delta} + D_m \cos \frac{\pi y}{\delta}\right) \sin \frac{m\pi x}{a}$$

It is shown in Appendix A that each D_m can be expressed in terms of all the C_m's so that ultimately the condition for instability can be written in terms of the C_m's alone. This condition is system (20). The determinant of this system also factors into two parts, one in which m is even and one in which m is odd. These two determinants always have exactly the same root L_{cr}. Accordingly, the curves for this report were made using the even determinant.

Note that each off-diagonal term in the determinant of system (20) is itself an infinite sum over r. Accuracy to within 0.1 percent could be maintained in the range $0 \leq S_x < S_{x1}$ by taking 4 terms in each off-diagonal sum and using a 4×4 determinant.

There was no need to optimally select important terms in this analysis because the variation in the shape of the buckle is accounted for by $\frac{\delta}{a}$. For each panel, $\frac{\delta}{a}$ was chosen by trial so as to minimize L_{cr}. The dependence of L_{cr} on $\frac{\delta}{a}$ turned out to be roughly parabolic (Appendix B and fig. 3).

---

[4]Underlined numbers in parenthesis refer to Literature Cited at end of this report.

How to Use the Curves

The curves in figures 4 through 8 are plotted from formulas (9) and (10) and show the buckling coefficient, L_{cr}, in terms of the aspect ratio $\frac{a}{b}$, and the parameters S_x and t. All of the curves on a single sheet correspond to the same choice of facing materials; that is, they have the same set of values for α_1, β_1, γ_1, α_2, β_2, and γ_2. In addition, the same choice of facing materials always appears on figures 4, 5, and 6 corresponding to $\theta = 0.4$, 1.0, and 2.5. These values of θ were chosen so that the curves would apply to hexagonal honeycomb and isotropic cores.

Each figure shows a family of curves depending on the parameter S_x, of which five members are shown, corresponding to $S_x = 0$, 0.05, 0.1, 0.2, and 0.4.

This range is sufficient to include most practical sandwich constructions. Each member of this family is further shown as a subfamily of curves depending on t, of which from two to four members are shown. The curves for $t = 0$ represent a panel with similar facings having the properties of facing 1, and the curves for $t = 1$ represent a panel with similar facings having the properties of facing 2.

Note that if the panel has dissimilar facings ($0 < t < 1$), one of type 1 and the other of type 2, the theoretical buckling load factor always lies between those for panels with similar facings of type 1 and type 2. The curves indicate that one could interpolate linearly with respect to t with very little error, so that the only curves needed to design panels with dissimilar facings are the two for similar facings of type 1 and type 2.

Accordingly, the curves in figures 7 and 8 are plotted for similar orthotropic facings only. Furthermore, only three values of S_x are used. If intermediate values of S_x are desired, a plot of L_{cr} versus S_x must be drawn from the three values of S_x provided.

The computed data from which figures 7 and 8 were constructed do not provide sufficient information to draw cusped curves. The location of the cusps shifted unexpectedly with a change in the value of the parameter α. Since the cusps are known to be very shallow, it was decided to draw the approximate envelope as a dashed line and omit cusps on these curves. For each value of S_x, the

uppermost curve shows both the envelope and the computer output on three branches, where the middle branch corresponds to m + n odd.

The values of α, β, and γ that were used in this report apply approximately to most of the glass-fabric laminates listed in table 1 of Forest Products Laboratory Report No. 1867 (7), and exactly to isotropic facings whose Poisson's ratio is 1/4.

The computer output from which the design curves were constructed is given in tables 1 and 2. These values are probably accurate to within 1 percent (Appendix B).

Finite or Infinite Panel, All Edges Clamped, $0 \leq S < S_1$

Only similar isotropic facings and isotropic cores are considered. Let L_o be the value of L_{cr} at $S = 0$. When $S = 0$, the core shear rigidity is infinite, plane transverse cross sections of the panel remain plane during bending, and the sandwich can be treated as a homogeneous plate whose bending stiffness is that of the spaced facings, namely

$$D = \frac{E_f}{1 - \sigma_f^2} \frac{f_1 f_2 h^2}{f_1 + f_2}, \quad h = c + \frac{f_1 + f_2}{2} \quad . \tag{22}$$

In this manner, values of L_o can be obtained from the literature in this field and a curve of L_o versus $\frac{a}{b}$ as computed by Smith (9) for clamped panels is given in figure 9. Also included in figure 9, for comparison, is a curve for L_o, from formula 9, for simply supported panels.

For values of S in the range $0 \leq S < S_1$ L_{cr} can be approximated with a fair degree of accuracy by

$$L_{cr} = \frac{L_o}{1 + \frac{S}{S_1}(L_o S_1 - 1)}, \quad 0 \leq S < S_1 \tag{23}$$

This formula was constructed so as to make $L_{cr} = L_o$ at $S = 0$ and $L_{cr} = \frac{1}{S_1}$ at $S = S_1$. For $S \geq S_1$, $L_{cr} = \frac{1}{S}$. A more exact mathematical analysis of the clamped panel is given in Appendix A. Computations made with that method indicate that formula (23) is reliable at $\frac{a}{b} = 0$ and $\frac{a}{b} = 1$; the reliability of the formula has not been established for values of $\frac{a}{b}$ between these two. A method by which an estimate of the buckling load can be made on the basis of formula (23) when the facings are stressed beyond their proportional limit is described in the analysis of test results.

Experimental Investigation

Introduction

Much work has been done at the Forest Products Laboratory to determine the behavior of flat plywood panels when subjected to shear. An approximate extension of the plywood theories and experimental techniques to sandwich construction was made in 1947. In contrast to the specimens of the present study, the specimens used in that early work were thin and were large in size, and because of that, the buckling loads were not adversely affected by shearing deformations in the core. The agreement of the test results for sandwich panels with the extended plywood theory was not good. The reasons suggested were that in the tests, the edge conditions were not properly controlled, and that the framework that applied the loads may not have been sufficiently rigid and may have influenced the results considerably. It was observed also that many of the specimens failed by sudden crimping before the load-deflection curves showed evidence that buckling had occurred.

The present type of specimen is shown in figure 10. Plywood loading rails were bonded to both facings at all four edges of the panels. The corners of the panel were cut so that there was approximately 1/8-inch clearance between the nearest corners of adjacent edge rails. Cut-out corners were curved to minimize stress concentrations. The testing arrangement that was used for the plywood panels, and also for the early sandwich work, was designed to induce shear in the panel by means of a compression type of loading apparatus. Subsequently it was discovered that a tension type of apparatus would develop the same quality of shear and would also produce greater buckling loads than would apparatus of the compression type. The compression arrangement was unsatisfactory because it tended to amplify initial eccentricities and, for that

reason, gave low results. The tension apparatus was more convenient and avoided the danger of including eccentricities. Therefore all the test results included in this report were obtained from tests in the tension type of apparatus.

It was discovered that the compression at the loaded corner was much greater than that needed to produce pure shear in the panel at that location. This would cause failure of panels at low loads, particularly if the panel was of a construction likely to crimp just as buckling of the entire panel would occur. This condition was corrected by changing the angle of the force applied to the rails. The change was made by increasing the length of the loading links until the strains at the corner showed that pure shear was being developed.

Description of Materials

Facings. --Panel facings consisted of clad aluminum alloy 24S-T3 in thicknesses of either 0.012, 0.020, or 0.032 inch. The facings on any one panel were of the same thickness.

Cores. --The core materials were not isotropic in the usual sense, but were isotropic to the extent that the shear modulus was the same or nearly the same in directions parallel and perpendicular to a side of the panel. This would not be true of all core materials, particularly the present type of honeycomb cores. The following core materials were used in this study:

Cores of end-grain balsa, grain direction normal to the facings of the sandwich, were made by edge-bonding 2- by 4-inch blocks with a thermosetting synthetic resin adhesive. The density range of the balsa was from 5 to 9 pounds per cubic foot.

Hard sponge rubber cores were of an expanded, hard, synthetic rubber. The cores were built up of strips approximately 2 inches wide edge-bonded with a thermosetting synthetic resin adhesive. The density of the cores was from 6.2 to 7.2 pounds per cubic foot.

Cores of corkboard sheet material were used in several panels for the purpose of obtaining a sandwich that had a core material with an extremely low modulus of rigidity. This material was obtained in three grades having moduli of rigidity of 1,500, 950, and 320 pounds per square inch. The corkboard was of the type commonly used for bulletin boards.

Bonding. --The facings were bonded to the cores in a two-stage process. The primary adhesive used on all facing was a high-temperature-setting mixture of thermosetting resin and synthetic rubber cured for 30 minutes at 325° F.

The secondary adhesive (used to bond the facings to the balsa cores) was a high-temperature-setting, acid-catalyzed, phenol-resin cured in a hot press at 230° F. and 75 pounds per square inch for 1 hour.

This same secondary adhesive was used for panels with hard sponge rubber cores with the exception that the pressure was 12 pounds per square inch instead of 75 pounds per square inch.

Facings were bonded to the corkboard cores with a secondary adhesive of a room-temperature-setting, resorcinol resin, cured in a press at room temperature and 14 pounds per square inch for 8 hours.

The loading rails, of 1- or 1-1/2-inch birch plywood 4 inches wide, were bonded to the facings with a room-temperature-setting, resorcinol resin, cured in a press at room temperature for 8 hours at the appropriate pressures corresponding to those used to bond the facings to the cores.

Methods of Testing

The panels were tested in a hydraulic testing machine, as shown in figure 10. Pins placed near the ends of the loading rails were loaded through links attached to a central loading pin at each end of the vertical diagonal of the specimen. The central loading pins were held in eyebolts that were supported in a spherical seat in the upper and lower heads of the testing machine. The entire arrangement was constructed so as to prevent eccentricity of load application. A sketch in figure 11 shows the exact panel size and position of pins.

In order to prevent local instability, 1- by 4-inch wood strips were clamped on each side of the loading rails near the upper and lower ends of the specimen. These strips were placed perpendicular to the direction of the applied load so as to restrain the specimen to its plane shape during the test, thereby decreasing the effects of eccentricities in the specimen itself.

Lateral deflection at the center of the panel was measured by means of a dial gage.

The panels, which had cores of 1/8-inch nominal thickness, were tested with the angle of the loading links at 45° to the vertical. Those panels buckled as a whole, and no failures were attributed to local compression concentrations near the loaded ends. The panels with 1/4-inch balsa cores were tested with the loading links at an angle of 35.5° to the vertical. This position of the links was found after several trials at angles between 0° and 45°. The correct angle was determined by observing the strains on each facing at the corner for various angles and finally choosing the one that produced pure shear. Additional

gages were placed elsewhere in the panel to check the quality of the shear. The strains were measured by means of 1-inch electric strain gages bonded to each facing as near to the edge rail as possible. Strains in three directions were measured at each location, thus enabling the shear to be computed at various points throughout the panel.

Results of the study to determine the proper direction of load to produce pure shear at the loaded corner are presented in figure 12. The strains at the corner of panel 121 are represented in strain circle diagrams for the various angles at which the load was applied. The diagram depicting the load applied at 45° to the vertical ($\theta = 45°$) shows that the compression strain was approximately 60 percent larger than required to produce pure shear. Pure shear was produced for $\theta = 35.5°$. Loads applied at angles less than 35.5° produced extensions greater than needed for pure shear, but the unbalance was not so severe compared with the compression illustration even to $\theta = 0°$. A similar panel failed at about one-half the load for $\theta = 45°$ than for $\theta = 35.5°$.

The results of an additional test to determine the quality of shear at various locations on panel 121 are presented in figure 13. As before, the measured strains are represented in strain circle diagrams. The strain circles at a panel load of 20,000 pounds show that pure shear existed at the loaded corner, that there was a slight excess of extension at the free corner, and that central portions of the panel were subjected to nearly pure shear. By discounting the small concentration of strain at the free corner, the entire panel was considered to be subjected to pure shear.

Results of Tests

The panel dimensions, buckling loads, and maximum loads are given in table 3.

The buckling loads were determined by examining the load-deflection curves, or load-strain curves for changes in shape as the load was increased. Sudden increases in deflections or strains indicated that the buckling load had been reached. Observations of the specimen during the test also gave a reasonable indication of the load at which buckling occurred. The facing stresses at these buckling loads were computed by the formula

$$q'_f = \frac{P}{2f\sqrt{a^2 + b^2}}$$

where

P -- buckling load

f -- facing thickness

a -- panel width

b -- panel length (for the panels tested b = a

$$\text{and } q'_f = \frac{P}{2\sqrt{2}\,fa})$$

Final failure of the panels occurred at or slightly above the buckling load. These failures occurred suddenly and were usually of the crimping type caused by sudden shear failure of the core due to the high stresses induced by the buckle. Although approximately half of the panels failed at loads greater than necessary to cause buckling, the greatest difference between any maximum load and the corresponding buckling load was only 30 percent. Buckling of these panels under static load might precipitate failure at the buckling load rather than allow the panels to carry additional load, as they did in the testing machine.

Analysis of Test Results

A discussion of the mathematical analysis for the buckling of flat panels of isotropic sandwich construction has been given previously. The results for simply supported panels are contained in the curves of figures 4 through 8 and for clamped panels in approximate formula (23). The formula for the facing stress at which the panel will buckle is

$$q_f = \frac{N_{cr}}{f_1 + f_2} = \frac{\pi^2 E_f f_1 f_2 h^2}{a^2 \lambda_f (f_1 + f_2)^2} \cdot L_{cr} \tag{24}$$

where

$$h = c + \frac{f_1 + f_2}{2}$$

c -- core thickness

f_1, f_2 -- facing thicknesses

a -- width of panel

b -- length of panel

$$\lambda_f = 1 - \sigma_f^2$$

σ_f -- Poisson's ratio of facings

For simply supported panels,

$$L_{cr} = \begin{cases} \text{value taken from figure 4, } S < \dfrac{1}{1 + \dfrac{a^2}{b^2}} \\ \dfrac{1}{S}, \quad S \geq \dfrac{1}{1 + \dfrac{a^2}{b^2}} \end{cases}$$

For clamped panels,

$$L_{cr} = \begin{cases} \dfrac{L_o}{1 + \left[L_o - \frac{4}{3}\left(1 + \frac{a^2}{b^2}\right)\right] S}, \quad S < \dfrac{\frac{3}{4}}{1 + \dfrac{a^2}{b^2}} \\ \dfrac{1}{S}, \quad S \geq \dfrac{\frac{3}{4}}{1 + \dfrac{a^2}{b^2}} \end{cases} \tag{25}$$

E_f -- compressive modulus of elasticity of the facings

$$S = \frac{\pi^2 c f_1 f_2 E_f}{a^2 \lambda_f \mu_c (f_1 + f_2)}$$

μ_c -- shear modulus of the core

Note whenever $L_{cr} = \frac{1}{S}$ $\quad q_f = \dfrac{h^2 \mu_c}{c(f_1 + f_2)} \approx \dfrac{h \mu_c}{f_1 + f_2}$

Values of L_o were taken from the literature in this field and are presented in figure 9. For square panels with edges clamped, $L_o = 14.7$.

In order to establish the theory as a criterion for the performance of sandwich panels in shear, experimental values of the buckling factor were plotted against values of S in figure 14. Since S depends upon the modulus of elasticity of the facings, the only test results that could be plotted were those in which the proportional limit stress was not exceeded, because the modulus of elasticity above proportional limit stress values was not readily determined without consideration of the panel edge conditions. A later paragraph will be devoted to behavior above proportional limit stress values. The value of S also depends upon the shear modulus of the core. The shearing moduli are given in table 3. The values used here were established by previous tests of the same kinds of core materials.

Examination of the points and curves shown in figure 14 shows that the curves fairly well represent the experimental points. The points for the most part lie in the region of the curve for plates with clamped edges and the curve for plates with edges simply supported in what is probably the practical range for S, that is, for values less than 0.4. For values of S greater than 0.4 the experimental points lie above the theoretical curve. The stiffnesses of the individual facings were not included in the calculations for this curve. If these stiffnesses are included, the theoretical values will be increased. This increase is greater for large values of S than for small values. It was found by computation that the theoretical value for the construction represented by the point near S = 4 was approximately doubled when the stiffness of the individual facings was taken into account. The inclusion of the stiffness of the individual facings in the calculations requires a separate curve for each particular sandwich construction.

A few panels were tested in which buckling occurred at facing stresses greater than the compressive, proportional-limit stress. Since the compressive and tensile stresses developed in the facings of the panel are equal to the shear stress, it was considered that the facing properties controlling the behavior were the compressive properties because the proportional limit stress in compression is lower than that in tension. It was also assumed that the modulus of elasticity of the facings decreased the same amount in all directions at stresses greater than the compressive, proportional-limit value. The modulus of elasticity at stresses greater than the compressive proportional limit stress was assumed to be the "tangent modulus," which is defined as the slope of the stress-strain curve at any stress.

Expressions for behavior of isotropic sandwich constructions at stresses greater than the proportional limit were obtained as follows. Approximate formula (23) was used to account for the dependence of L_{cr} upon S for simply supported panels by taking

$$S_1 = \frac{1}{1 + \frac{a^2}{b^2}}$$

so that, for simple support,

$$L_{cr} \approx \frac{L_o}{1 + S\left[L_o - \left(1 + \frac{a^2}{b^2}\right)\right]}, \quad 0 \leq S \leq \frac{1}{1 + \frac{a^2}{b^2}} \tag{26}$$

Taking the reciprocal of equation (24) and substituting for L_{cr},

$$\frac{1}{q_f} \approx \frac{a^2 \lambda_f (f_1 + f_2)^2}{\pi^2 E_f f_1 f_2 h^2 L_o} + \frac{c(f_1 + f_2)\left[L_o - \left(1 + \frac{a^2}{b^2}\right)\right]}{\mu_c h^2 L_o} \tag{27}$$

Here L_o is the value of L_{cr} at $S = 0$ for simply supported panels and can be obtained from figure 4. Since the facings are assumed to be thin, $\frac{c}{h}$ can be cancelled in the second term of equation (27). The assumption that the tangent modulus is to be used leads to

$$\frac{1}{q_f} \approx \frac{a^2 \lambda_f (f_1 + f_2)^2}{\pi^2 E_{ft} f_1 f_2 h^2 L_o} + \frac{(f_1 + f_2)\left[\left[L_o - \left(1 + \frac{a^2}{b^2}\right)\right]\right]}{\mu_c h L_o}$$

Multiplying both sides by the Young's modulus of elasticity, $\underline{E_f}$

$$\frac{E_f}{q_f} = A \frac{E_f}{E_{ft}} + B$$

where

$$A = \frac{a^2 \lambda_f (f_1 + f_2)^2}{\pi^2 f_1 f_2 h^2 L_o}$$

$$B = \frac{(f_1 + f_2)\left[L_o - \left(1 + \frac{a^2}{b^2}\right)\right]}{\mu_c h L_o}$$

$$\text{for } S < \frac{1}{1 + \frac{a^2}{b^2}}$$

where

$$S = \frac{\pi^2 f_1 f_2 E_f}{a^2 h \mu_c (f_1 + f_2)} \qquad (28)$$

This straight line can be plotted on the same sheet with a curve, as shown in in figure 15, $\frac{E_f}{q_f}$ versus $\frac{E_f}{E_{ft}}$ constructed from the stress strain data for the facing material. Since $\underline{q_f}$ and $\underline{E_{ft}}$ at buckling must be compatible with the stress strain curve, the intersection of these two curves gives the critical buckling stress.

The data for the last two specimens given in table 3 were analyzed by means of equation (28). The edges of the panels were assumed to be simply supported. The computed buckling stresses were nearly identical with the experimental values. An additional column in table 3 gives these computed values.

Conclusions

The mathematical analysis fairly well represents the stability behavior of square, flat panels of symmetrical, isotropic, sandwich constructions subjected to pure shear. The testing techniques described will produce nearly pure shear in square, flat, panels of symmetrical, isotropic, sandwich constructions.

The elastic buckling load of simply supported rectangular sandwich panels with dissimilar facings when subjected to pure shear can be obtained from the design curves and formulas (1) through (4).

The plastic buckling stress in the facings of a flat panel of symmetrical, isotropic, sandwich construction can be estimated as follows:

1. Determine values of the parameter $\underline{L_o}$ from the curves of figure 9, after considerations as to edge conditions and size of panel.

2. With these values and the construction dimensions and properties, use equation (28) to determine the straight line to be drawn on a graph similar to figure 15.

3. The value of the ordinate at the intersection of this straight line with the curve similar to figure 15 will give the facing stress if it is divided into the Young's modulus of the facing material.

4. If a panel is to be designed, the above procedure can be reversed. A stress would be known; therefore, a modulus is known. Then equation (28) can be solved for the core thickness or shear modulus or whatever else is to be found.

APPENDIX A

Mathematical Analysis of the Shear Stability of Flat Sandwich Panels

Flat simply supported sandwich panels with dissimilar orthotropic facings of unequal thickness and orthotropic cores are analyzed in sections A 1 through A 3 by energy methods. Clamped panels with similar isotropic facings of unequal thickness and isotropic cores are analyzed in sections A 4 through A 6 by the differential equations method of Libove and Batdorf (6).

A 1. Finite Dissimilar Panels, Simply Supported

The lateral deflection is assumed to be a double sine series

$$w = \sum_{m=1} \sum_{n=1} w_{mn} \tag{A 1}$$

with

$$w_{mn} = C_{mn} \sin \frac{m \pi x}{a} \sin \frac{n \pi y}{b} \tag{A 2}$$

where x and y are coordinates with axes taken in two of the edges of the panel. The x, y plane is fixed at the juncture of the core and the facing of thickness f_1 and the y axis is taken as shown in figure 1. The letters a and b designate the dimensions of the panel with a measured along the x-axis, c designates the thickness of the core, and f_2 the thickness of the second facing.

Expression(A 1) is taken for the deflection throughout the thickness of the panel.

In the analysis it is assumed that the core and facing materials are orthotropic. Two of the orthotropic axes of these materials are assumed to be parallel to the edges of the panel and the third perpendicular to the facings.

The core is assumed to be antiplane. That is, the transverse shear stresses are constant throughout its thickness and its bending energy may be neglected.

To this end, the components of displacement in the core are taken as double infinite sums, over m and n, of

$$\left.\begin{aligned} u_{C_{mn}} &= (k_{mn}\, z + q_{mn}) \frac{\partial w_{mn}}{\partial x} \\ v_{C_{mn}} &= (h_{mn}\, z + r_{mn}) \frac{\partial w_{mn}}{\partial y} \end{aligned}\right\} \qquad \text{(A 3)}$$

The constants k_{mn}, q_{mn}, h_{mn}, and r_{mn} are chosen so as to minimize the total potential energy of the loaded sandwich panel. This method is a generalization of that used in references (4), (5), and (11).

The continuity of displacements at the glue lines prescribes that the components (A 3) evaluated at z = 0 and z = c shall be those of the inner surfaces of facing 1 and facing 2, respectively. Within each facing, the components of displacement are assumed to be such that sections originally plane and perpendicular to the middle surface of the facing remain plane and perpendicular to the deformed middle surface. Accordingly, the components of displacement in facing 1 and facing 2 are taken as double infinite sums, over m and n, of

$$\left.\begin{aligned} u_{1_{mn}} &= (q_{mn} - z) \frac{\partial w_{mn}}{\partial x} \\ v_{1_{mn}} &= (r_{mn} - z) \frac{\partial w_{mn}}{\partial y} \\ u_{2_{mn}} &= (k_{mn}\, c + q_{mn} - z + c) \frac{\partial w_{mn}}{\partial x} \\ v_{2_{mn}} &= (h_{mn}\, c + r_{mn} - z + c) \frac{\partial w_{mn}}{\partial y} \end{aligned}\right\} \qquad \text{(A 4)}$$

The components of strain with core or facing will be denoted by the superscripts c, 1, and 2. Summation over the subscripts m and n is implied.

$$e_{zx}^{(c)} = (1 + k_{mn}) \frac{\partial w_{mn}}{\partial x}, \quad e_{yz}^{(c)} = (1 + h_{mn}) \frac{\partial w_{mn}}{\partial y} \qquad \text{(A 5)}$$

The remaining strains in the core are neglected.

It is convenient to consider the components of strain in the facings as the superposition of two states of strain. The first of these consists of the membrane strains or strains in their middle surfaces:

$$\left.\begin{aligned}
e^{(1)}_{xx_{mn}} &= \left(q_{mn} + \frac{f_1}{2}\right) \frac{\partial^2 w_{mn}}{\partial x^2} \\
e^{(1)}_{yy_{mn}} &= \left(r_{mn} + \frac{f_1}{2}\right) \frac{\partial^2 w_{mn}}{\partial y^2} \\
e^{(1)}_{xy_{mn}} &= \left(q_{mn} + r_{mn} + f_1\right) \frac{\partial^2 w_{mn}}{\partial x \partial y} \\
e^{(2)}_{xx_{mn}} &= \left(k_{mn} c + q_{mn} + \frac{f_2}{2}\right) \frac{\partial^2 w_{mn}}{\partial x^2} \\
e^{(2)}_{yy_{mn}} &= \left(h_{mn} c + r_{mn} + \frac{f_2}{2}\right) \frac{\partial^2 w_{mn}}{\partial y^2} \\
e^{(2)}_{xy_{mn}} &= \left(k_{mn} c + q_{mn} + h_{mn} c + r_{mn} + f_2\right) \frac{\partial^2 w_{mn}}{\partial x \partial y}
\end{aligned}\right\} \quad \text{(A 6)}$$

The second state of strain in the facings is that associated with the bending of the facings about their own middle surfaces. This state, in either facing, has the components

$$\left.\begin{aligned}
e'_{xx_{mn}} &= - z' \frac{\partial^2 w_{mn}}{\partial x^2} \\
e'_{yy_{mn}} &= - z' \frac{\partial^2 w_{mn}}{\partial y^2} \\
e'_{xy_{mn}} &= - 2z' \frac{\partial^2 w_{mn}}{\partial x \partial y}
\end{aligned}\right\} \quad \text{(A 7)}$$

where $\underline{z'}$ is measured from the middle surface of the facing.

The strain energy of the core or facings is given by

$$\left.\begin{aligned} U = \frac{1}{2\lambda}\int_V [\, & E_x\, e_{xx}^2 + E_y\, e_{yy}^2 + 2\, E_x\, \sigma_{yx}\, e_{xx}\, e_{yy} \\ & + \lambda\, \mu_{xy}\, e_{xy}^2 + \lambda\, \mu_{yz}\, e_{yz}^2 + \lambda\, \mu_{zx}\, e_{zx}^2 \,]\, dV \end{aligned}\right\} \quad \text{(A 8)}$$

where, for the material under consideration (core or facing), $\lambda = 1 - \sigma_{yx}\, \sigma_{xy}$, E_x and E_y are Young's moduli, μ_{xy}, μ_{yz}, and μ_{zx} are moduli of rigidity, and σ_{yx} and σ_{xy} are Poisson's ratios. Primed letters will denote the elastic constants of the core material, and unprimed letters with subscript i = 1, 2 will denote those of the facing materials. The integration in formula (A 8) is to be carried out over the entire volume of the core or facing.

The total strain energy of the panel can finally be expressed in the form

$$U = \frac{b\pi^2}{8a} \sum_{m=1} \sum_{n=1} T_{mn}\, C_{mn}^2 \qquad \text{(A 9)}$$

where T_{mn} is a quadratic in k_{mn}, h_{mn}, q_{mn}, and r_{mn}. This method is found in Forest Products Laboratory Reports Nos. 1583-C (1) and 1583-B (2).

Let N_{xy} designate the shear force per inch of edge applied to the edges of the panel. It is assumed that N_{xy} is constant over the edges of the panel and that no other loads are applied. The work done by the applied load is then

$$U_L = N_{xy} \int_0^a \int_0^b \frac{\partial w}{\partial x}\, \frac{\partial w}{\partial y}\, dy\, dx \qquad \text{(A 10)}$$

With the substitution of (A 1) and (A 2) for $\underline{w}$, it is found that

$$U_L = -\frac{\pi^2 N_{xy}}{8} \sum_{m=1} \sum_{n=1} \sum_{r=1} \sum_{s=1} C_{mn} C_{rs} H_{mn}^{rs} \qquad \text{(A 11)}$$

where

$$H_{mn}^{rs} = \frac{32\, m\, n\, r\, s}{\pi^2 (m^2 - r^2)(n^2 - s^2)} \text{ if } m + r \text{ and } n + s \text{ are odd}$$

$$= 0 \text{ if } m + r \text{ or } n + s \text{ are even} \qquad \text{(A 12)}$$

The total potential energy of the panel is

$$W = U - U_L$$

or, with the use of equations (A 9) and (A 10)

$$W = \frac{b\pi^2}{8a} \sum_{m=1} \sum_{n=1} T_{mn} C_{mn}^2 + \frac{\pi^2 N_{xy}}{8} \sum_{m=1} \sum_{n=1} \sum_{r=1} \sum_{s=1} C_{mn} C_{rs} H_{mn}^{rs} \qquad \text{(A 13)}$$

This expression depends upon the undetermined parameters $\underline{C_{mn}}$, $\underline{q_{mn}}$, $\underline{r_{mn}}$, $\underline{k_{mn}}$, and $\underline{h_{mn}}$, the last four of which appear in the expression $\underline{T_{mn}}$. These five sets of parameters are determined by imposing the conditions

$$\frac{\partial w}{\partial C_{mn}} = 0, \quad \frac{\partial T_{mn}}{\partial (q_{mn})} = 0, \quad \frac{\partial T_{mn}}{\partial (h_{mn})} = 0, \quad \frac{\partial T_{mn}}{\partial k_{mn}} = 0, \quad \frac{\partial T_{mn}}{\partial h_{mn}} = 0$$

The first of these conditions yields

$$\frac{b}{a} T_{mn} C_{mn} + N_{xy} \sum_{r=1} \sum_{s=1} C_{rs} H_{mn}^{rs} = 0 \quad m, n = 1, 2, 3, \text{-----}$$

Let $\underline{T'_{mn}}$ designate the expression for $\underline{T_{mn}}$ after imposing the last four conditions. Then upon imposing all five conditions

$$\frac{b}{a} T'_{mn} C_{mn} + N_{xy} \sum_{r=1} \sum_{s=1} C_{rs} H^{rs}_{mn} = 0 \quad m, n = 1, 2, 3 \text{ ----- } \quad \text{(A 14)}$$

An expression for $\underline{T'_{mn}}$ may be given in terms of the eight physical constants

$$\left.\begin{aligned}
\alpha_i &= \sqrt{\frac{E_{xi}}{E_{yi}}} \\
\beta_i &= \frac{\lambda_i}{\sqrt{E_{xi} E_{yi}}} \left\{ \frac{E_{xi} \sigma_{yxi}}{\lambda_i} + 2\mu_{xyi} \right\} \quad i = 1, 2 \\
\gamma_i &= \frac{\lambda_i \mu_{xyi}}{\sqrt{E_{xi} E_{yi}}} \\
S_x &= \frac{c}{h^2 \mu'_{zx}} \cdot D \frac{\pi^2}{a^2} \\
S_y &= \frac{c}{h^2 \mu'_{yz}} \cdot D \frac{\pi^2}{a^2}
\end{aligned}\right\} \quad \text{(A 15)}$$

and the expressions

$$\left.\begin{aligned}
D &= \frac{T_1 T_2 h^2}{T_1 + T_2} \\
T_i &= \frac{\sqrt{E_{xi} E_{yi}}}{\lambda_i} f_i, \quad i = 1, 2 \\
h &= c + \frac{1}{2}(f_1 + f_2)
\end{aligned}\right\} \quad \text{(A 16)}$$

$$D_f^{(i)} = \frac{f_i^2 \; T_i}{12} \; , \qquad i = 1, \; 2$$

$$t = \frac{T_1}{T_1 + T_2} \qquad \text{(A 16)}$$

This expression is

$$T'_{mn} = D \; \frac{\pi^2}{a^2} \; [\; V_{mn}^{(1)} + V_{mn}^{(2)} + V_{mn} \;] \qquad \text{(A 17)}$$

where

$$V_{mn}^{(i)} = \frac{D_f^{(i)}}{D} \; K_{mn}^{(i)} \qquad i = 1, \; 2 \qquad \text{(A 18)}$$

$$K_{mn}^{(i)} = \alpha_i \; m^4 + 2\beta_i \; \frac{m^2 n^2 a^2}{b^2} + \frac{1}{\alpha_i} \; \frac{n^4 a^4}{b^4} \; , \quad i = 1, \; 2 \qquad \text{(A 19)}$$

and

$$V_{mn} = \frac{t \; F_{mn}^{(1)} \; K_{mn}^{(2)} + (1-t) \; F_{mn}^{(2)} \; K_{mn}^{(1)} + (\frac{n^2 a^2}{b^2} \; S_y + m^2 S_x) \; F_{mn}^{(1)} \; F_{mn}^{(2)}}{\psi_{mn} + [\; t \; F_{mn}^{(1)} \; L_{mn}^{(2)} + (1-t) \; F_{mn}^{(2)} \; L_{mn}^{(1)} \;] \; S_x + S_x \; S_y \; F_{mn}^{(1)} \; F_{mn}^{(2)}}$$

with

$$\psi_{mn} = t^2 \; F_{mn}^{(1)} + 2 \; t \; (1 - t) \; F_{mn}^{(12)} + (1 - t)^2 \; F_{mn}^{(2)}$$

$$\left.\begin{aligned} L_{mn}^{(i)} &= \alpha_i \; m^2 + \gamma_i \; \frac{n^2 a^2}{b^2} + \theta(\frac{1}{\alpha_i} \; \frac{n^2 a^2}{b^2} + \gamma_i \; m^2) \\ F_{mn}^{(i)} &= (1 - \beta_i^2) \; \frac{m^2 n^2 a^2}{b^2} + \gamma_i \; K_{mn}^{(i)} \end{aligned}\right\} \; i = 1, \; 2$$

$$F_{mn}^{(12)} = [\frac{1}{2} \; (\frac{\alpha_1}{\alpha_2} + \frac{\alpha_2}{\alpha_1}) - \beta_1 \; \beta_2] \; \frac{m^2 n^2 a^2}{b^2} + \frac{1}{2} [\gamma_1 K_{mn}^{(2)} + \gamma_2 \; K_{mn}^{(1)}] \qquad \text{(A 20)}$$

Let

$$L_{xy} = \frac{N_{xy} a^2}{D \pi^2} \tag{A 21}$$

Then with the substitution of (A 17) into (A 14), one obtains

$$\left(\frac{V_{mn}^{(1)} + V_{mn}^{(2)} + V_{mn}}{\frac{a}{b} L_{xy}} \right) C_{mn} + \sum_{r=1} \sum_{s=1} H_{mn}^{rs} C_{rs} = 0, \; m, n = 1, 2, \ldots \tag{A 22}$$

The expression $V_{mn}^{(i)}$ accounts for the effect of the bending of a facing about its own middle surface. This effect is usually neglected because it is assumed that the facings are thin.

The solution $C_{mn} = 0$, all m and n, is the one which holds for arbitrary values of L_{xy} below the critical load. At the instant of buckling, however, the lateral deflection is nonzero. The condition that system (A 22) have a nonzero solution is that its determinant must vanish; this condition determines two values of L_{xy} since the determinant separates into two factors, one in which m + n is even and the other in which m + n is odd. The critical buckling constant, L_{cr}, is the smaller of the two. The critical shear force is then

$$N_{cr} = D \frac{\pi^2}{a^2} L_{cr} \tag{A 23}$$

A 2. Infinite Panels Dissimilar Facings, Simply Supported[5]

The lateral deflection is taken in the form

$$w = \sum_{m=1} \left(C_m \sin \frac{\pi y}{\delta} + D_m \cos \frac{\pi y}{\delta}\right) \sin \frac{m\pi x}{a} \qquad \text{(A 24)}$$

where δ is the half wave length of a longitudinal normal section of the panel. It is again assumed that the deflection is constant throughout the thickness of the panel.

The strain energy in a section of the panel of length δ associated with either of the two terms in (A 24) may be obtained from formula (A 9) by taking the single term n = 1 in the summation over n and by replacing b by δ and C_{m1} by C_m or D_m. Since the energies associated with the two terms are additive, the strain energy in the sandwich is

$$U = \frac{\delta \pi^2}{8a} \sum_{m=1} T_{m1} \left(C_m^2 + D_m^2\right) \qquad \text{(A 25)}$$

where T_{m1} denotes T_{mn} of formula (A 9) with n = 1 and b replaced by δ.

An expression for the work done by an applied uniform shear force N_{xy} on a section of the panel of length δ is obtained by substituting (A 24) into (A 10) and integrating over an interval of length δ in place of b. This leads to

$$U_L = -\frac{\pi^2}{8} N_{xy} \sum_{m=1} \sum_{r=1} \left\{C_r D_m - C_m D_r\right\} H_m^r \qquad \text{(A 26)}$$

---

[5]This case has been discussed by Seide (8) for sandwich with equal facings.

where

$$\left.\begin{aligned} H_m^r &= \frac{8\,m\,r}{\pi\,(m^2 - r^2)} \quad \text{for } m + r \text{ odd} \\ &= 0 \quad \text{for } m + r \text{ even} \end{aligned}\right\} \tag{A 27}$$

From formulas (A 25) and (A 26) the total potential energy in the sandwich, $U - U_L$, is

$$W = \frac{\delta\pi^2}{8\,a} \sum_{m=1} T_{ml} \left\{ C_m^2 + D_m^2 \right\} + \frac{\pi^2 N_{xy}}{8} \sum_{m=1} \sum_{r=1} \left\{ C_r D_m - C_m D_r \right\} H_m^r \tag{A28}$$

For the determination of the parameters $\underline{C_m}$, $\underline{D_m}$, $\underline{q_{ml}}$, $\underline{r_{ml}}$, $\underline{k_{ml}}$, and $\underline{h_{ml}}$, the last four sets of which appear in $\underline{T_{ml}}$, the conditions $\frac{\partial w}{\partial C_m} = 0$, $\frac{\partial w}{\partial D_m} = 0$, $\frac{\partial T_{ml}}{\partial q_{ml}} = 0$, $\frac{\partial T_{ml}}{\partial r_{ml}} = 0$, $\frac{\partial T_{ml}}{\partial k_{ml}} = 0$, $\frac{\partial T_{ml}}{\partial h_{ml}} = 0$ are imposed. The first two of these yield

$$\frac{\delta}{a}\, T_{ml}\, C_m - N_{xy} \sum_{r=1} D_r\, H_m^r = 0, \quad m = 1,\ 2,\ ---- \tag{A 29}$$

and

$$\frac{\delta}{a}\, T_{ml}\, D_m + N_{xy} \sum_{r=1} C_r\, H_m^r = 0, \quad m = 1,\ 2,\ ---- \tag{A 30}$$

respectively. Let $\underline{T'_{ml}}$ designate the expression for $\underline{T_{ml}}$ after imposing the last four conditions. The two preceding equations with $\underline{T'_{ml}}$ substituted for $\underline{T_{ml}}$ then result from imposing all conditions. After making this modification change $\underline{r}$ to $\underline{s}$ and then $\underline{m}$ to $\underline{r}$ throughout formula (A 30) and substitute the

expression for D_r obtained in this manner into (A 29). Then

$$C_m + \frac{a^2}{\delta^2} N_{xy}^2 \sum_{r=1} \sum_{s=1} \frac{C_s H_m^r H_r^s}{T'_{m1} T'_{r1}} = 0, \quad m = 1, 2, 3, \text{----}$$

With the substitution of expressions obtained from (A 17) for T'_{m1} and T'_{r1} and with the use of (A 21),

$$\frac{(V_{m1}^{(1)} + V_{m1}^{(2)} + V_{m1}) \frac{\delta}{a}}{L_{xy}^2} C_m - \sum_{s=1} \left\{ \sum_{r=1} \frac{H_s^r H_m^r}{(V_{r1}^{(1)} + V_{r1}^{(2)} + V_{r1}) \frac{\delta}{a}} \right\} C_s = 0$$

$$s = 1, 2, 3, \ldots \qquad \text{(A 31)}$$

where $V_{m1}^{(i)}$, $i = 1, 2$, and V_{m1} are obtained from $V_{mn}^{(i)}$ and V_{mn} by setting $n = 1$ and substituting δ for b. This system of equations breaks down into two parts, one in which m is odd and one in which m is even. The critical shear force is obtained from L_{cr}, which is the smaller value of L_{xy} at which one or the other of the determinants of the two systems vanishes. The terms $V_{m1}^{(i)}$ and $V_{r1}^{(i)}$, $i = 1, 2$, may be neglected if the facings are thin.

A 3. Limiting Behavior When S_x is Large; Simple Support

It has been reported by Seide (8); that, when S is sufficiently large, for isotropic sandwich constructions

$$L_{cr} = \frac{1}{S}$$

The deflected surface is characterized by buckles of short wave length and straight nodal lines. This type of instability, which is associated with

transverse shear deformations of the core, will now be established for panels with dissimilar orthotropic facings and orthotropic cores.

For the case of a finite rectangular panel, the deflection is taken as

$$w = C \sin \frac{\pi x}{a} \sin \frac{\pi y}{b} \cos \frac{n\pi}{b} (y + \eta x) \tag{A 32}$$

For the case of an infinitely long panel, the deflection is taken as

$$w = C \sin \frac{\pi x}{a} \sin \frac{\pi}{\delta} (y + \eta x) \tag{A 33}$$

In these expressions, $\underline{\eta}$ is the slope of the nodal lines, $\underline{n}$ is an integer denoting the number of buckles in a finite panel, and $\underline{\delta}$ is the half wave length of a buckle in an infinitely long panel. These parameters will be chosen so as to minimize the total potential energy of the loaded panel.

A possible source of error in results obtained by the use of the above expression is that the condition that the bending moments vanish on the edges of the panel cannot be satisfied. In the case of an infinitely long panel where (A 33) is used the errors so introduced are not large. When $\underline{S}$ is large it is expected that results obtained by the use of formula (A 32) will also be in good approximation to those obtained by more exact methods.

An expression for the critical shear load, when $\underline{w}$ is of the form given by (A 32) or (A 33), can be obtained by making modifications in the formulas of section A 1. Simply drop the subscripts $\underline{m}$ and $\underline{n}$ so that $w_{mn} = w$ and $\underline{w}$ is given by

(A 32) or (A 33). Then the total strain energy of the panel can be expressed in the form

$$\begin{aligned} U = {} & B_1 q^2 + 2B_2 q r + B_3 r^2 \\ & + 2B_4 q k + 2B_5 (q h + r k) + 2B_6 r h \\ & + B_7 k^2 + 2B_8 k h + B_9 h^2 \\ & + 2B_{10} q + 2B_{11} r + 2B_{12} k + 2B_{13} h \\ & + B_{14} + B_{15} \end{aligned} \tag{A 34}$$

where the B_j, $j = 1, 15$ are given in Forest Products Laboratory Report No. 1583-B (2) by formulas (A 19) and (A 17) with w taken as (A 32) or (A 33) of this report.

The work done by a shear force of N_{xy} pound per inch of edge is given by (A 10).

The condition for instability is

$$U_L = U \tag{A 35}$$

or

$$N_{xy} = U' \tag{A 36}$$

where

$$U' = \frac{U}{\int_0^a \int_0^b \frac{\partial w}{\partial x} \frac{\partial w}{\partial y} \, dy \, dx} \tag{A 37}$$

It is convenient to let

$$B_j' = \frac{B_j}{\int_0^a \int_0^b \frac{\partial w}{\partial x} \frac{\partial w}{\partial y} \, dy \, dx}, \quad j = 1, \ldots, 15 \tag{A 38}$$

so that U' is given by (A 34) by simply inserting primes.

The conditions

$$\frac{\partial N_{xy}}{\partial q} = 0, \quad \frac{\partial N_{xy}}{\partial r} = 0, \quad \frac{\partial N_{xy}}{\partial k} = 0, \quad \frac{\partial N_{xy}}{\partial h} = 0$$

are now imposed for the determination of q, r, k, and h. These yield equations (A 26) of reference (2). When solving those equations for q, r, k, and h and substituting their values into (A 36), it is found that

$$N_{xy} = \frac{\begin{vmatrix} B'_1 & B'_2 & B'_4 & B'_5 & B'_{10} \\ B'_2 & B'_3 & B'_5 & B'_6 & B'_{11} \\ B'_4 & B'_5 & B'_7 & B'_8 & B'_{12} \\ B'_5 & B'_6 & B'_8 & B'_9 & B'_{13} \\ B'_{10} & B'_{11} & B'_{12} & B'_{13} & B'_{14} \end{vmatrix}}{\begin{vmatrix} B'_1 & B'_2 & B'_4 & B'_5 \\ B'_2 & B'_3 & B'_5 & B'_6 \\ B'_4 & B'_5 & B'_7 & B'_8 \\ B'_5 & B'_6 & B'_8 & B'_9 \end{vmatrix}} + B'_{15} \tag{A 39}$$

These determinants can be evaluated by the process given in Appendix C of reference (2). The term B'_{15} represents the effect of the bending of the facings about their own middle surfaces and is hereafter neglected.

The condition for instability (A 36) can be reduced to dimensionless form by defining L_{cr} as in (A 21), and by introducing the notation

$$\left.\begin{aligned} c_1 &= \frac{\int_0^a \int_0^b \left(\frac{\partial^2 w}{\partial x^2}\right)^2 dy\, dx}{\frac{2\pi^2}{a^2} \int_0^a \int_0^b \frac{\partial w}{\partial x} \frac{\partial w}{\partial y}\, dy\, dx} \\ c_2 &= \frac{\int_0^a \int_0^b \left(\frac{\partial^2 w}{\partial x \partial y}\right)^2 dy\, dx}{\frac{2\pi^2}{a^2} \int_0^a \int_0^b \frac{\partial w}{\partial x} \frac{\partial w}{\partial y}\, dy\, dx} \end{aligned}\right\} \tag{A 40}$$

$$
\left.
\begin{aligned}
c_3 &= \frac{\displaystyle\int_0^a \int_0^b \left(\frac{\partial^2 w}{\partial y^2}\right)^2 \, dy \, dx}{\dfrac{2\pi^2}{a^2} \displaystyle\int_0^a \int_0^b \frac{\partial w}{\partial x} \frac{\partial w}{\partial y} \, dy \, dx} \\[2ex]
c_4 &= \frac{\displaystyle\int_0^a \int_0^b \left(\frac{\partial w}{\partial x}\right)^2 \, dy \, dx}{2 \displaystyle\int_0^a \int_0^b \frac{\partial w}{\partial x} \frac{\partial w}{\partial y} \, dy \, dx} \\[2ex]
c_5 &= \frac{\displaystyle\int_0^a \int_0^b \left(\frac{\partial w}{\partial y}\right)^2 \, dy \, dx}{2 \displaystyle\int_0^a \int_0^b \frac{\partial w}{\partial x} \frac{\partial w}{\partial y} \, dy \, dx}
\end{aligned}
\right\} \qquad \text{(A 40)}
$$

In this notation, (A 36) becomes

$$
L_{cr} = \frac{t F_1 K_2 + (1-t) F_2 K_1 + \left(\dfrac{S_x}{c_4} + \dfrac{S_y}{c_5}\right) F_1 F_2}{\psi_1 + \left[t F_1 L_2 + (1-t) F_2 L_1\right] \dfrac{S_x}{c_4} + \dfrac{S_x S_y}{c_4 c_5} F_1 F_2} \qquad \text{(A 41)}
$$

where

$$
\left.
\begin{aligned}
\psi_1 &= t^2 F_1 + 2t(1-t) F_{12} + (1-t)^2 F_2 \\[2ex]
\left.
\begin{aligned}
K_i &= \alpha_i c_1 + 2\beta_i c_2 + \frac{c_3}{\alpha_i} \\[2ex]
L_i &= \alpha_i c_1 + \gamma_i c_2 + \theta \frac{c_4}{c_5} \left(\frac{c_3}{\alpha_i} + \gamma_i c_2\right) \\[2ex]
F_i &= c_1 c_3 - \beta_i^2 c_2^2 + \gamma_i c_2 K_i
\end{aligned}
\right\} & i = 1, 2
\end{aligned}
\right\} \qquad \text{(A 42)}
$$

$$F_{12} = \frac{1}{2}\left(\frac{\alpha_1}{\alpha_2} + \frac{\alpha_2}{\alpha_1}\right) c_1 c_3 - \beta_1 \beta_2 c_2^2 + \frac{c_2}{2}(\gamma_1 K_2 + \gamma_2 K_1) \qquad \text{(A 42)}$$

For the finite rectangular panel, $\underline{w}$ is given by (A 32) so that

$$c_1 = \frac{\left(1 + n^2 \frac{a^2 \eta^2}{b^2}\right)^2 + 4n^2 \frac{a^2 \eta^2}{b^2}}{2n^2 \frac{a^2}{b^2} \eta}$$

$$c_2 = \frac{\frac{a^2}{b^2}\left(1 + n^2 \frac{a^2 \eta^2}{b^2}\right)(1 + n^2)}{2n^2 \frac{a^2}{b^2} \eta}$$

$$c_3 = \frac{\frac{a^4}{b^4}(1 + n^2)^2 + 4n^2}{2n^2 \frac{a^2}{b^2} \eta} \qquad \text{(A 43)}$$

$$c_4 = \frac{1 + n^2 \frac{a^2}{b^2} \eta^2}{2n^2 \frac{a^2}{b^2} \eta}$$

$$c_5 = \frac{\frac{a^2}{b^2}(1 + n^2)}{2n^2 \frac{a^2}{b^2} \eta}$$

Examination of the terms in L_{cr} given by (A 41) reveals that n never occurs to a degree higher than n^8 and the only eighth degree terms are the $F_1 F_2$ terms. Hence, as n becomes large, these terms dominate and L_{cr} becomes

$$L_{cr} = \frac{\frac{2 S_x}{\eta} + 2\eta S_y}{4 S_x S_y} = \frac{1 + \theta \eta^2}{2 \theta \eta S_x}$$

The slope of the buckles, η, is now adjusted so as to minimize L_{cr}. Setting

$$\frac{\partial L_{cr}}{\partial \eta} = 0$$

yields $\eta = \theta^{-\frac{1}{2}}$ so that

$$L_{cr} = \frac{1}{\sqrt{S_x S_y}} \tag{A 44}$$

when n, the number of buckles, is infinite.

When n is finite, L_{cr} is given by (A 41). One can find the least value of S_x for which (A 44) is applicable by imposing the condition that (A 44) is less than (A 41), letting n approach infinity, putting $\eta = \theta^{-\frac{1}{2}}$, and solving the inequality for S_x. The general result is rather cumbersome and is not given here but the resulting inequality for constructions with similar isotropic facings and orthotropic cores is

$$S_x \geq = \frac{\left(\frac{1 - \sigma_f}{2}\right) 4 \theta + (1 - \theta)^2}{\left(\frac{1 - \sigma_f}{2}\right) (1 + \theta)^2 \left[\theta + \frac{a^2}{b^2}\right]} \tag{A 45}$$

where σ_f is Poisson's ratio of the facing material. If the core is also isotropic, $\theta = 1$ and this result reduces to

$$S \geq S_1 = \frac{1}{1 + \frac{a^2}{b^2}} \tag{A 46}$$

When $S_x < S_{x1}$ the errors in this analysis that arise from the failure to satisfy the conditions of simple support exactly become worse as S_x becomes small, and the Fourier Series method of section (A 1) gives better results. If (A 41) is to be applied in the range $0 \leq S_x < S_{x1}$, however, then the integer n must be chosen by trial so as to minimize L_{cr}. This yields a scalloped curve, whereas the exact curve obtained by Fourier Series is smooth (fig. 16).

For the infinitely long panel, w is given by (A 33) and from (A 40)

$$\left.\begin{aligned}
c_1 &= \frac{\left(1 + \frac{a^2}{\delta^2}\eta^2\right)^2 + 4\frac{a^2}{\delta^2}\eta^2}{2\frac{a^2}{\delta^2}\eta} \\
c_2 &= \frac{\frac{a^2}{\delta^2}\left(1 + \frac{a^2}{\delta^2}\eta^2\right)}{2\frac{a^2}{\delta^2}\eta} \\
c_3 &= \frac{\frac{a^4}{\delta^4}}{2\frac{a^2}{\delta^2}\eta}
\end{aligned}\right\} \tag{A 47}$$

$$c_4 = \frac{1 + \frac{a^2}{\delta^2}\eta^2}{2\frac{a^2}{\delta^2}\eta}$$

$$c_5 = \frac{1}{2\eta} \qquad \text{(A 47)}$$

Again L_{cr} is given by (A 41) except that now, for the infinite case, the c_j, $j = 1, \ldots, 5$ are given by (A 47). Again, the $F_1 F_2$ terms dominate the expression for L_{cr} as $\frac{a}{\delta}$ approaches infinity; that is, as the half wave length becomes shorter, again the best $\eta = \theta^{-\frac{1}{2}}$, and the same limit, (A 44), results. Formula (A 44) yields lower values of L_{cr} than (A 41) if $S_x \geq S_{x1}$ where S_{x1} can be obtained by the method outlined above. For sandwich constructions with similar isotropic facings and orthotropic cores

$$S_{x1} = \frac{\left(\frac{1 - \sigma_f}{2}\right) 4\theta + (1 - \theta)^2}{\left(\frac{1 - \sigma_f}{2}\right) (1 + \theta)^2 \theta} \qquad \text{(A 48)}$$

If the core is also isotropic

$$S_1 = 1 \qquad \text{(A 49)}$$

Formulas (A 48) and (A 49) seem reasonable since they follow from (A 45) and (A 46), respectively, in the limit as $\frac{a}{b}$ approaches zero.

A 4. Finite Isotropic Panels, All Edges Clamped

The equations of equilibrium of a panel subjected to shear force of intensity N_{xy} units per inch of edge may be given in the forms ((6) pages 13 and 14).

$$\left.\begin{aligned}
&2 N_{xy} \frac{\partial^2 w}{\partial x \partial y} + \frac{\partial Q_x}{\partial x} + \frac{\partial Q_y}{\partial y} = 0 \\
&- D \frac{\partial}{\partial x}\left(\frac{\partial^2 w}{\partial x^2} + \frac{\partial^2 w}{\partial y^2}\right) + \frac{(1-\sigma)D}{2 D_Q} \frac{\partial^2 Q_x}{\partial y^2} + \frac{D}{D_Q} \frac{\partial^2 Q_x}{\partial x^2} - Q_x + \frac{(1-\sigma)D}{2 D_Q} \frac{\partial^2 Q_y}{\partial x \partial y} = 0 \\
&- D \frac{\partial}{\partial y}\left(\frac{\partial^2 w}{\partial x^2} + \frac{\partial^2 w}{\partial y^2}\right) + \frac{(1-\sigma)D}{2 D_Q} \frac{\partial^2 Q_y}{\partial x^2} + \frac{D}{D_Q} \frac{\partial^2 Q_y}{\partial y^2} - Q_y + \frac{(1-\sigma)D}{2 D_Q} \frac{\partial^2 Q_x}{\partial x \partial y} = 0
\end{aligned}\right\} \quad \text{(A 50)}$$

In these equations the symbols σ, D, and D_Q denote, respectively, the Poisson ratio of the facings, the flexural stiffness, and the shear stiffness of the sandwich. It is assumed that the core and facing materials are isotropic, and that the effects of the bending of the facings about their own middle surfaces can be neglected. Consequently, it is assumed that

$$D = \frac{E_f}{\lambda_f} \frac{f_1 f_2}{(f_1 + f_2)} \left(c + \frac{f_1 + f_2}{2}\right)^2 \qquad \text{(A 51)}$$

and

$$D_Q = \frac{\left(c + \frac{f_1 + f_2}{2}\right)^2}{c} \mu_c \qquad \text{(A 52)}$$

These formulas are consistent with those developed in section A 1 of this appendix.

For a complete solution of the system (A 50), three conditions are imposed at each edge. In the present discussion, however, an approximate solution is given. This solution, obtained from the work of Green and Hearmon (3), is one in which the boundary conditions imposed are those of ordinary plate theory. When S = 0, these boundary conditions are the correct ones, and the results are expected to be consistent with those obtained in ordinary isotropic

plate theory. On the other hand, when $\underline{S}$ is large, it is shown in the following section that since the facings are considered as membranes, the critical load is determined by the criterion (A 44) as in the case of simple support. Under the present assumptions, therefore, the effect of taking the boundary conditions as those of ordinary plate theory is to introduce errors in a range of moderate values of $\underline{S}$.

In order to obtain an equation to which the solution of Green and Hearmon is applicable, differentiate the second of equations (A 50) once with respect to $\underline{x}$ and add to the result the third equation of the same set after differentiating it once with respect to $\underline{y}$. The resulting equation is one in $\underline{w}$ and $\frac{\partial Q_x}{\partial x} + \frac{\partial Q_y}{\partial y}$.

Then using the first equation of the set to eliminate the latter variable one obtains

$$D\left\{\frac{\partial^4 w}{\partial x^4} + \frac{2\partial^4 w}{\partial x^2 \partial y^2} + \frac{\partial^4 w}{\partial y^4}\right\} + \frac{2 D N_{xy}}{D_Q}\frac{\partial^4 w}{\partial x^3 \partial y} + \frac{2 D N_{xy}}{D_Q}\frac{\partial^4 w}{\partial x \partial y^3}$$

$$- 2 N_{xy}\frac{\partial^2 w}{\partial x \partial y} = 0 \qquad \text{(A 53)}$$

In their discussion of the buckling of plywood plates Green and Hearmon have applied the following equilibrium equation

$$D_{11}\frac{\partial^4 w}{\partial x^4} + 2\left(D_{12} + 2 D_{66}\right)\frac{\partial^4 w}{\partial x^2 \partial y^2} + D_{22}\frac{\partial^4 w}{\partial y^4} + 4 D_{16}\frac{\partial^4 w}{\partial x^3 \partial y}$$

$$+ 4 D_{26}\frac{\partial^4 w}{\partial x \partial y^3} + P_1\frac{\partial^2 w}{\partial x^2} + P_2\frac{\partial^2 w}{\partial y^2} + 2 P_{12}\frac{\partial^2 w}{\partial x \partial y} = 0 \qquad \text{(A 54)}$$

((3) equation 2. 2). This equation is identical with (A 53) provided

$$\left.\begin{aligned} D_{11} &= D_{12} + 2\,D_{66} = D_{22} = D \\ D_{16} &= D_{26} = \frac{N_{xy}\,D}{2\,D_Q} \\ P_{12} &= -\,N_{xy} \\ P_1 &= P_2 = 0 \end{aligned}\right\} \quad \text{(A 55)}$$

With these substitutions, the criterion for instability derived by Green and Hearmon is applicable in the present case. Accordingly, the critical shear stress is determined by the condition that the determinant of the following system of equations vanish ((3) equations 7. 7 to 7. 18).

$$\sum_{r=1} \sum_{s=1} \alpha_{rsmn}\, A_{rs} = 0 \quad m,\ n = 1,\ 2,\ 3\text{----} \qquad \text{(A 56)}$$

where

$$\left.\begin{aligned} \rho &= \frac{a}{b} \\ \alpha_{11\,11} &= 12 + 8\,\rho^2 + 12\rho^4 \\ \alpha_{1s1s} &= 8 + 4\,\rho^2\,(s^2 + 1) + \frac{3\rho^4}{2}\,(s^4 + 6s^2 + 1),\ s \neq 1 \\ \alpha_{r1r1} &= \frac{3}{2}\,(r^4 + 6r^2 + 1) + 4\rho^2\,(r^2 + 1) + 8\rho^4,\ r \neq 1 \end{aligned}\right\} \quad \text{(A 57)}$$

$$\alpha_{rsrs} = r^4 + 6r^2 + 1 + 2\rho^2 (r^2 + 1)(s^2 + 1) + \rho^4 (s^4 + 6s^2 + 1) \ , \qquad r \neq 1, \ s \neq 1$$

$$\alpha_{rsmn} = - \left\{ \frac{(r+1)^4}{2} + \rho^2 (r+1)^2 (s^2 + 1) + \frac{\rho^4}{2} (s^4 + 6s^2 + 1) \right\}, \qquad m = r + 2, \ n = s \neq 1$$

$$= - \left\{ \frac{3(r+1)^4}{4} + 2\rho^2 (r+1)^2 + 4\rho^4 \right\}, \quad m = r + 2, \ n = s = 1$$

$$= - \left\{ \frac{(r^4 + 6r^2 + 1)}{2} + \rho^2 (r^2 + 1)(s+1)^2 + \frac{\rho^4}{2} (s+1)^4 \right\}, \qquad m = r \neq 1, \ n = s + 2$$

$$= - \left\{ 4 + 2\rho^2 (s+1)^2 + \frac{3\rho^4}{4} (s+1)^4 \right\}, \quad m = r = 1, \ n = s + 2$$

$$= \frac{1}{4} \left\{ (r+1)^2 + \rho^2 (s+1)^2 \right\}^2, \quad m = r + 2, \ n = s + 2$$

$$\alpha_{rsmn} = \frac{1}{4} \left\{ (r+1)^2 + \rho^2 (s+1)^2 \right\}^2, \quad m = r + 2, \ s = n + 2 \qquad \text{(A 57)}$$

$$= - (16)^3 \rho_{rsmn} L_{xy} \left\{ (r^2 + m^2 - 2)(s^2 + n^2 - 2) \right.$$

$$+ 2S (r^2 + m^2 + r^2 m^2 - 3)(s^2 + n^2 - 2)$$

$$\left. + 2S\rho^2 (r^2 + m^2 - 2)(s^2 + n^2 + n^2 s^2 - 3) \right\}$$

$$\div 2\pi^2 (r^2 - m^2)(s^2 - n^2) \left\{ (r-2)^2 - m^2 \right\} \left\{ (r+2)^2 - m^2 \right\} \left\{ (s-2)^2 - n^2 \right\} \left\{ (s+2)^2 - n^2 \right\}$$

$$\left.\begin{array}{c} r + m \text{ and } s + n \text{ odd} \\ \alpha_{mnrs} = \alpha_{rsmn} \end{array}\right\} \quad (A\ 57)$$

Here the notation

$$\left.\begin{array}{l} L_{xy} = \dfrac{N_{xy}\, a^2}{D\, \pi^2} \\ S = \dfrac{\pi^2}{a^2}\, \dfrac{D}{D_Q} \end{array}\right\} \quad (A\ 58)$$

which, according to formulas (A 51) and (A 52), is consistent with (A 15) and (A 21), has been used.

The system of equations (A 56) separates into two parts, one in which r + s are odd numbers in the other r + s are even numbers. Consequently, two determinants must be considered and the critical stress is obtained from the smaller L_{xy} for which one or the other vanishes.

A 5. Infinite Isotropic Panels, All Edges Clamped

The buckling load of an infinitely long plywood panel has been discussed by Green and Hearmon, and their criterion for instability is made applicable to the present case by the substitution (A 55). Thus, the critical shear load is determined by the condition that the determinant of the system ((3) equation 8.6)

$$\sum_{r=1}^{\infty} \alpha_{rm} A_r = 0, \quad m = 1, 2, 3---- \quad (A\ 59)$$

vanish. The coefficients α_{rm} are given as follows ((3) equations 8.7 to 8.12)

$$\left.\begin{array}{l} \alpha_{rr} = r^4 - \dfrac{8r^2}{\pi^2} + 2\mu^2\left(\dfrac{5r^2}{3} - \dfrac{16}{\pi^2}\right) + \mu^4\left(1 + \dfrac{\pi^2 r^2}{15} - \dfrac{16}{\pi^2 r^2}\right), \quad r \text{ odd} \\ \quad = r^4 - \dfrac{24r^2}{\pi^2} + 2\mu^2\left(\dfrac{7r^2}{5} - \dfrac{48}{\pi^2}\right) + \mu^4\left(1 + \dfrac{\pi^2 r^2}{105} - \dfrac{48}{\pi^2 r^2}\right), \quad r \text{ even} \end{array}\right\} \quad (A\ 60)$$

$$\alpha_{rm} = -\frac{8rm}{\pi^2} + 2\mu^2 \left\{\frac{2rm}{3} - \frac{8\,(r^2 + m^2)}{\pi^2 rm}\right\}$$

$$+ \mu^4 \left\{\frac{\pi^2 rm}{15} - \frac{8\,(r^4 + m^4)}{\pi^2 r^3 m^3}\right\} \qquad \text{r odd, m odd} \quad r \neq m$$

$$= -\frac{24rm}{\pi^2} + 2\mu^2 \left\{\frac{2rm}{5} - \frac{24\,(r^2 + m^2)}{\pi^2 rm}\right\}$$

$$+ \mu^4 \left\{\frac{\pi^2 rm}{105} - \frac{24\,(r^4 + m^4)}{\pi^2 r^3 m^3}\right\} \qquad \text{r even, m even} \quad r \neq m$$

$$\alpha_{rm} = \frac{4\,i\,\mu\,L_{xy}\,S}{\pi} \left\{\frac{24m}{\pi^2 r} + \frac{2\,m^3 r}{r^2 - m^2}\right\}$$

$$- \frac{4\,i\,\mu\,L_{xy}}{\pi}\,(1 + \mu^2 S) \left\{\frac{\pi^2 rm}{30} - \frac{24m}{\pi^2 r^2} - \frac{2\,(r^4 + m^4 - r^2 m^2)}{rm\,(r^2 - m^2)}\right\} \qquad \text{r odd, m even}$$

$$\alpha_{rm} = -\frac{4\,i\,\mu\,L_{xy}\,S}{\pi} \left\{\frac{24r}{\pi^2 m} + \frac{2\,m\,r^3}{m^2 - r^2}\right\}$$

$$+ \frac{4\,i\,\mu\,L_{xy}}{\pi}\,(1 + \mu^2 S) \left\{\frac{\pi^2 rm}{30} - \frac{24r}{\pi^2 m^3} + \frac{2\,(r^4 + m^4 - r^2 m^2)}{rm\,(r^2 - m^2)}\right\} \qquad \text{r even, m odd}$$

(A 60)

where

$$i = \sqrt{-1}$$

and μ denotes a real parameter, which is proportional to the wave length of a longitudinal section of the panel. The critical shear load is determined from the minimum L_{xy}, with respect to μ, for which the determinant of the system (A 59) vanishes.

A 6. Limiting Behavior When S is Large, All Edges Clamped

The method used in section A 3 can again be applied to derive formulas that are applicable when S is large. For the case of a finite rectangular panel with clamped edges, the deflection

$$w = C \sin^2 \frac{\pi x}{a} \sin^2 \frac{\pi y}{b} \cos \frac{n\pi}{b} (x + y) \tag{A 61}$$

is assumed. The slope of the buckles is assumed to be 45°. Then using formulas (A 40) for the determination of the c_j, $j = 1, \ldots, 5$, and substituting into (A 41) for L_{cr}, it is found that

$$L_{cr} = \frac{1}{S} \tag{A 62}$$

when

$$S \geq S_1 = \frac{\frac{3}{4}}{1 + \frac{a^2}{b^2}} \tag{A 63}$$

corresponding to n infinite.

For the infinitely long panel

$$w = C \sin^2 \frac{\pi x}{a} \cos \frac{\pi}{\delta} (y + x) \tag{A 64}$$

is the assumed deflection and, for $\frac{a}{\delta}$ infinite, formula (A 62) again gives L_{cr}

when

$$S \geq S_1 = \frac{3}{4} \tag{A 65}$$

which could also be obtained from (A 63) by letting $\frac{a}{b}$ approach zero.

APPENDIX B

Details of the Numerical Analysis

B 1. Finite Dissimilar Panels, Simply Supported

For each panel considered, 30 terms were optimally selected from the double infinite array of terms C_{mn}. The selection was made in the following way.

From the first 49 terms (all terms for which $m + n \leq 14$, $m + n$ even), the pair that yielded the lowest L_{cr} when used in a 2×2 determinant was found by trial. With these two terms, each of the remaining terms was used to compute L_{cr} from a 3×3 determinant and the one that yielded the lowest L_{cr} was determined. These three terms were assumed to be the most important. They were used to order the remaining terms on the basis of the value of L_{cr} that each yielded when taken with the three most important terms to form a 4×4 determinant.

The first 30 terms of that term order were then used in the computation for that panel.

Since the determinant of system (9) can be factored into the product of an even determinant ($m + n$ even) and an odd one, it was necessary to investigate both factors to see which yielded the lower theoretical buckling coefficient. Figure 2 shows the results of study made on a single panel. This behavior is typical of all the panels investigated in this report, and explains why the curves of L_{cr} versus $\frac{a}{b}$ are cusped. Note that the curve for each determinant is itself cusped, although no particular integer is associated with each branch between cusps. The portion of the curve (fig. 2) for $m + n$ odd between $\frac{a}{b} = .75$ and $\frac{a}{b} = 1$ is shown as a straight line, although not enough points were plotted in this range to establish the exact shape of the curve. The straight line is based on only three points, and may be a coincidence.

To determine the number of terms needed for accuracy, a panel with S_x nearly equal to S_{x1} and $\frac{a}{b} = 0.25$ was solved by using a varied number of terms drawn from among the first 81 terms. Thirty terms yielded results with an error of less than 1 percent. Equal accuracy could be obtained by drawing the best 30 terms from among the first 49 terms. The variation in L_{cr} with number of terms is shown by the following:

Finite Panel		Infinite Panel	
$\alpha_1 = \alpha_2 = \beta_1 = \beta_2 = 1$		$\alpha_1 = \alpha_2 = \beta_1 = \beta_2 = 1$	
$\gamma_1 = \gamma_2 = 0.375$		$\gamma_1 = \gamma_2 = 0.375$	
$\frac{a}{b} = \frac{1}{4}$		$\frac{a}{b} = 0$	
$\theta = 1 \quad S_x = 0.8$		$\theta = 1 \quad S_x = 0.8$	
L_{cr}	Number of Terms	L_{cr}^2	Number of Terms
1.641	4	1.5376	2
1.326	10	1.5323	3
1.309	15	1.5306	4
1.289	20	1.5296	10
1.282	25		
1.279	30		

The accuracy of this method improves as $\frac{a}{b}$ increases or S_x decreases, so all the design curves in this report are surely accurate to within 1 percent.

Section B 4 shows a block diagram of the computing method which resulted from the foregoing preliminary investigations.

B 2. Infinite Panels, Dissimilar Facings, Simply Supported

System (A 31) found in section A 2 also factors into an even and an odd determinant, but computations made with each of them agreed to five significant figures, so the odd determinant was discarded.

The results of an investigation of the number of terms required for accuracy was shown previously. Four terms are evidently sufficient to give accuracy comparable to that obtained for the finite panels.

The variation of L_{cr} with $\frac{\delta}{a}$ was investigated in detail for four panels. Figure 3 shows the four curves that were obtained. Since the curves are roughly parabolic, fairly good results can be obtained by fitting a parabola to three points corresponding to $\frac{\delta}{a} = 0.5$, 1.0, and 1.5. A highly accurate final result can then be secured by hunting in the neighborhood of the minimum of the fitted parabola. Section B 4 shows the computing method in detail.

B 3. Clamped Isotropic Panels

The methods of sections A 4 and A 5 were used to compute L_{cr} for square panels ($\frac{a}{b} = 1$) and infinitely long panels ($\frac{a}{b} = 0$). For the square panel, a 5×5 determinant composed of the coefficients of A_{11}, A_{22}, A_{13}, A_{31}, and A_{33} in equation (A 56) was used. At $S = 0$, $L_{cr} = 15.4$, which is about 5 percent higher than the value $L_{cr} = 14.7$ given by Smith (9) who used a 12×12 determinant. The value $L_{cr} = 2.96$ was obtained at $S = S_1 = 0.375$. This is about 10 percent higher than $L_{cr} = \frac{1}{S} = 2.67$. A curve constructed from the computed values is given in figure 17, which also shows formula (23) for comparison.

In the computations for the infinitely long panel a 3×3 determinant composed of the coefficients of A_1, A_2, and A_3 in equation (A 60) was used. The value $L_{cr} = 5.35$, which was obtained at $S = 0$, is the same as that obtained by

Smith (9). A computation at $S = 1$ gave $L_{cr} = 1.11$, which is 11 percent high. This point, however, is included in the range $S \geq 0.75$ where $L_{cr} = \frac{1}{S}$, and it is expected that the error at $S = 0.75$ would be somewhat smaller.

The above computations are compared with formula (23) in figure 17, which indicates that formula (23) gives values of L_{cr} that are conservative by as much as 10 percent in some ranges of S.

In order to estimate the accuracy of formula (28), which is based on formula (26), figure 16 shows a comparison of formula (26) with computed values of L_{cr} taken from the design curves for simply supported panels. The figure indicates that the formula is never more than 10 percent low.

B 4. Block Diagrams of Computer Programs

Program 1. Finite Dissimilar Panels, Simply Supported

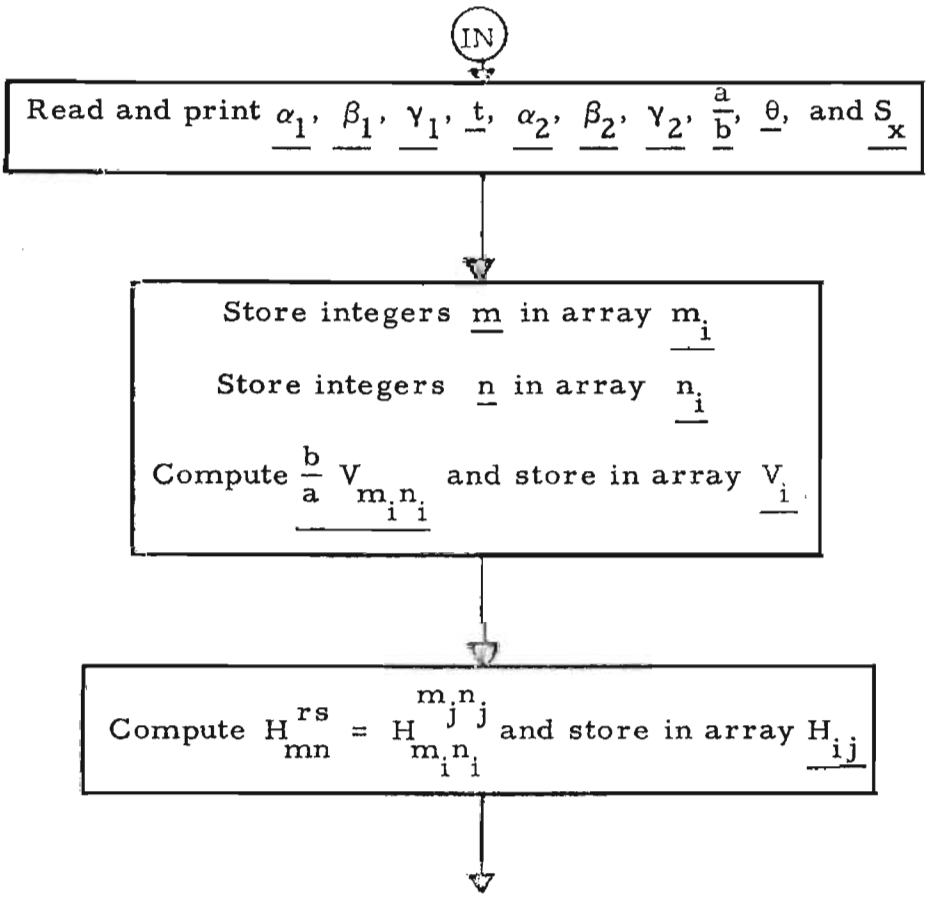

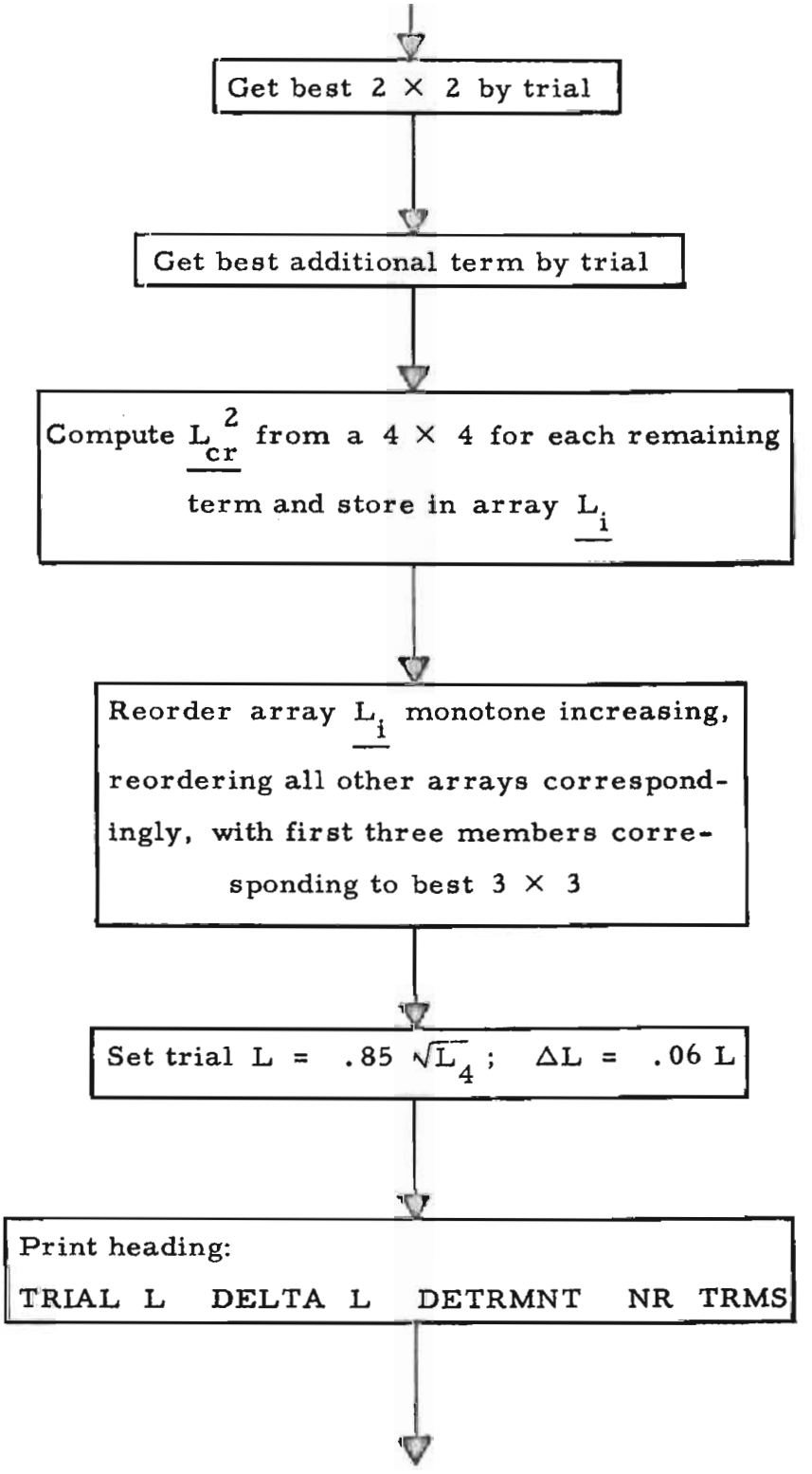
Get best 2 × 2 by trial
Get best additional term by trial
Compute L_{cr}^2 from a 4 × 4 for each remaining term and store in array L_i
Reorder array L_i monotone increasing, reordering all other arrays correspondingly, with first three members corresponding to best 3 × 3
Set trial L = .85 $\sqrt{L_4}$; ΔL = .06 L
Print heading:
TRIAL L DELTA L DETRMNT NR TRMS

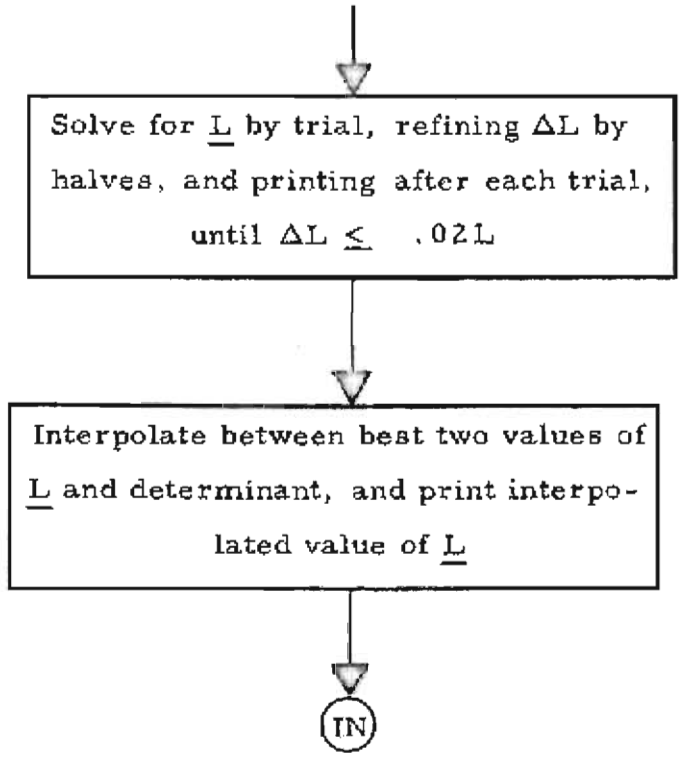

Program 2. Infinite Dissimilar Panels, Simply Supported

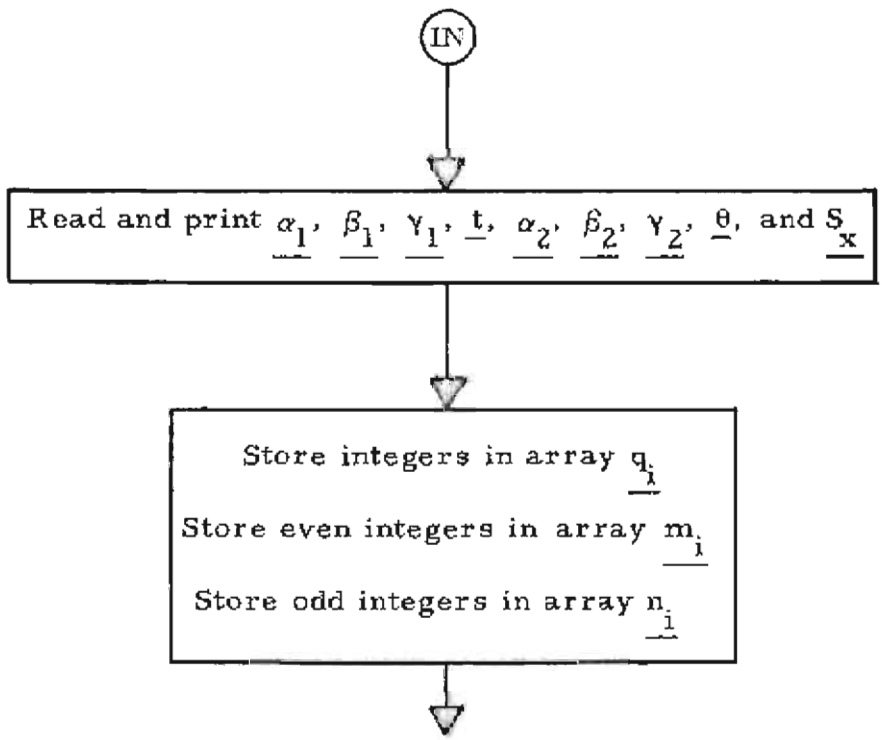

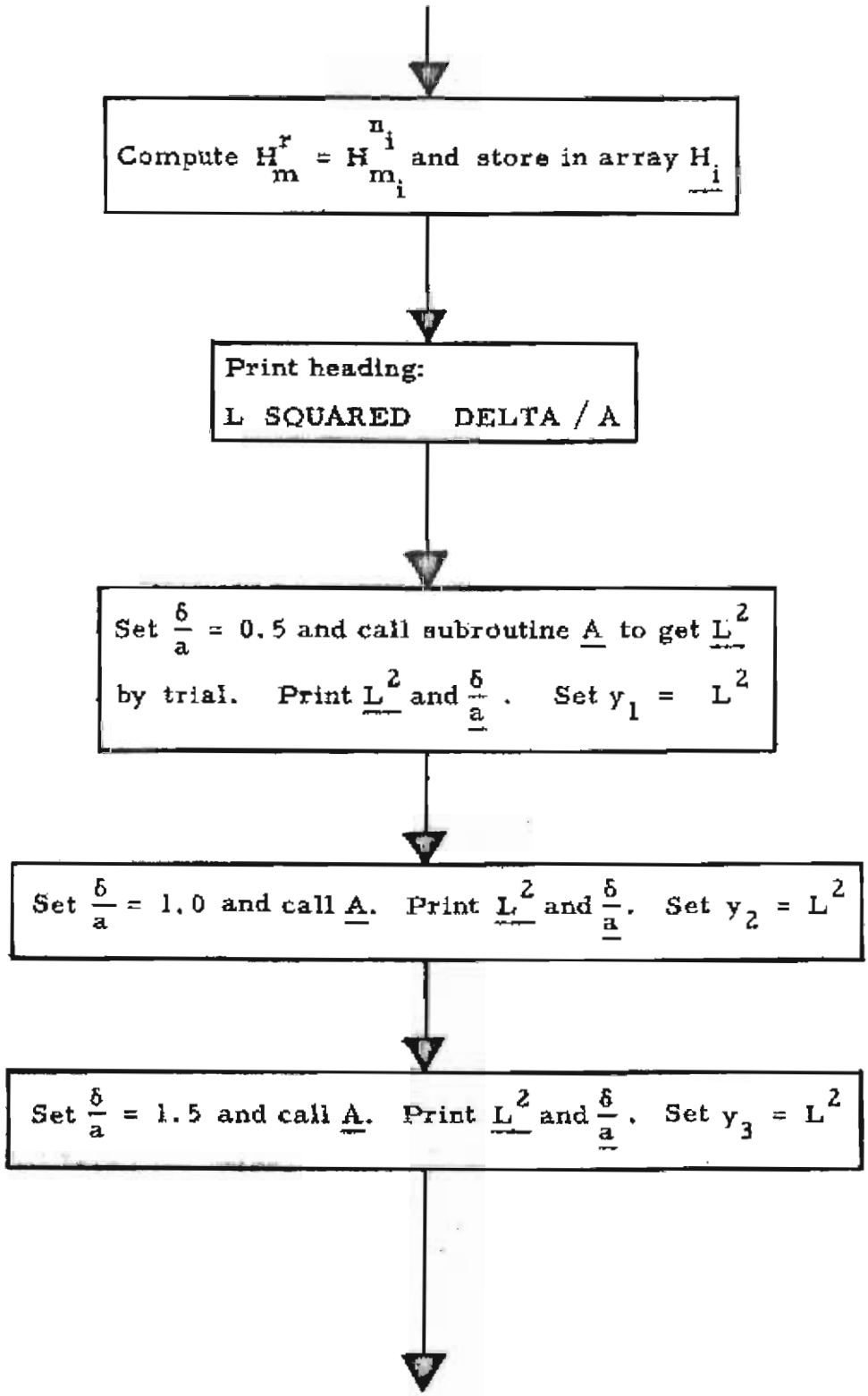
Compute $H_m^r = H_{m_i}^{n_i}$ and store in array $\underline{H_i}$
Print heading:
L SQUARED DELTA / A
Set $\frac{\delta}{a} = 0.5$ and call subroutine $\underline{A}$ to get $\underline{L^2}$ by trial. Print $\underline{L^2}$ and $\frac{\delta}{\underline{a}}$. Set $y_1 = L^2$
Set $\frac{\delta}{a} = 1.0$ and call $\underline{A}$. Print $\underline{L^2}$ and $\frac{\delta}{\underline{a}}$. Set $y_2 = L^2$
Set $\frac{\delta}{a} = 1.5$ and call $\underline{A}$. Print $\underline{L^2}$ and $\frac{\delta}{\underline{a}}$. Set $y_3 = L^2$

Set $\frac{\delta}{a} = \frac{2y_2 - \frac{1}{4}(3y_3 + 5y_1)}{2y_2 - y_3 - y_1}$. This locates the minimum point on a fitted parabola.

Call $\underline{A}$. Print $\underline{L^2}$ and $\underline{\frac{\delta}{a}}$. Set $y_4 = L^2$

Increment $\underline{\frac{\delta}{a}}$ by .05 and call $\underline{A}$. Print $\underline{L^2}$ and $\underline{\frac{\delta}{a}}$. Set $y_i = L^2$.

Iterate until $\underline{L^2}$ stops decreasing.

Find least value of $\underline{L^2}$ in array $\underline{y_i}$ and take square root.

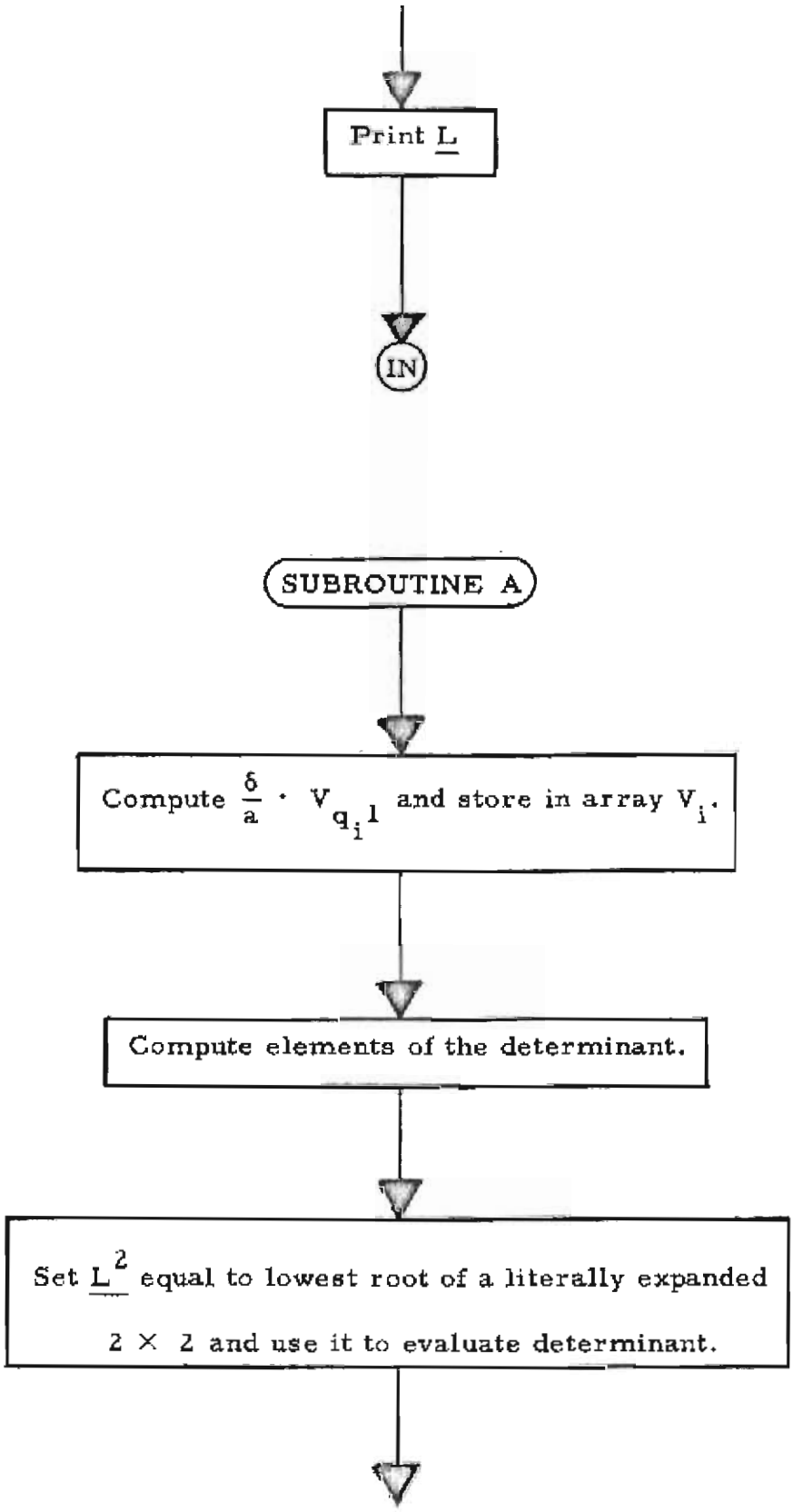
Print L
IN
SUBROUTINE A
Compute $\frac{\delta}{a} \cdot V_{q_i 1}$ and store in array V_i.
Compute elements of the determinant.
Set L^2 equal to lowest root of a literally expanded 2 × 2 and use it to evaluate determinant.

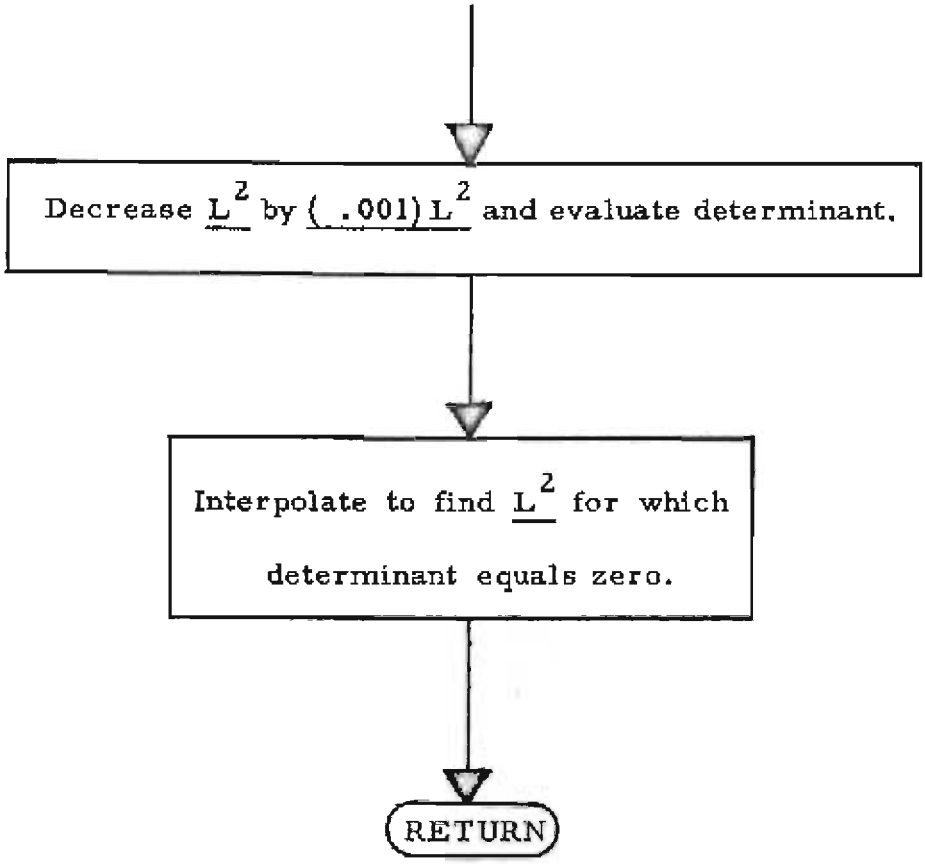
Decrease L^2 by $(.001)L^2$ and evaluate determinant.
Interpolate to find L^2 for which determinant equals zero.
RETURN

Literature Cited

(1) ERICKSEN, W. S.
1950. Deflection Under Uniform Load of Sandwich Panels Having Facings of Unequal Thickness. Forest Prod. Lab. Rept. No. 1583-C.

(2) _____, and MARCH, H. W.
1950. Compressive Buckling of Sandwich Panels Having Facings of Unequal Thickness. Forest Prod. Lab. Rept. No. 1583-B.

(3) GREEN, A. E., and HEARMON, R. F. S.
1945. The Buckling of Flat Rectangular Plywood Plates. Phil. Mag. Ser. 7, vol. xxxvi, p. 659, October.

(4) HOPKINS, H. G., and PEARSON, S.
1944. The Behavior of Flat Sandwich Panels Under Uniform Transverse Loading. Rept. No. S.M.E. 3277, Royal Aircraft Establishment, March.

(5) LEGGETT, D. M. A., and HOPKINS, H. G.
1944. Sandwich Panels and Cylinders Under Compressive End Loads. Rept. No. S.M.E. 3203, Royal Aircraft Establishment, March.

(6) LIBOVE, CHARLES, and BATDORF, S. B.
1948. A General Small-Deflection Theory for Flat Sandwich Plates. NACA T. N. No. 1526.

(7) NORRIS, C. B.
1958. Compressive Buckling Curves for Simply Supported Sandwich Panels With Glass-Fabric-Laminate Facings and Honeycomb Cores. Forest Prod. Lab. Rept. No. 1867.

(8) SEIDE, PAUL.
1949. Shear Buckling of Infinitely Long Simply Supported Metalite Type Sandwich Plates. NACA T. N. No. 1910, July.

(9) SMITH, R. C. T.
1946. The Buckling of Plywood Plates in Shear. A.C.A. Rept. SM 51.

(10) SEYDEL, E.
1933. Über das Ausbeulen von rechteckigen, isotropen oder orthogonal-anisotropen Platten bei Schubbeanspruchung. Ingenieur-Archiv. IV. Band.

(11) WILLIAMS, D., LEGGETT, D. M. A., and HOPKINS, H. G.
1941. Flat Sandwich Panels Under Compressive End Loads. Rept. No. A. D. 3174, Royal Aircraft Establishment, June.

Table 1.--Buckling coefficients for simply supported panels (computer output)

S_x	t \ a/b	L_{cr}										
			m + n even			m + n odd			m + n even			
		0	.167	.250	.333	.333	.417	.542	.500	.542	.750	1.000
		$\alpha_1 = 1,\ \beta_1 = 1,\ \gamma_1 = .375,\ \alpha_2 = 1,\ \beta_2 = 0.6,\ \gamma_2 = 0.2,\ \theta = 1$										
0	0	5.34		5.64		[1]5.85	[2]6.09		6.57		7.49	9.35
	1/3	5.04	5.18		5.60	5.51	5.74	6.44		6.27	6.97	8.66
	2/3	4.79	4.91		5.30	5.24	5.42	6.06		5.96	6.54	8.08
	1	4.58	[3]4.70	4.83	[1]5.03	[1]5.02	[2]5.13		5.66		6.18	7.57
.05	0	4.53		4.74			[2]5.04		5.41		5.95	7.01
	1/3	4.30	4.40		4.68	4.66	4.78	5.23		5.20	5.61	6.60
	2/3	4.11	4.21		4.46	4.46	4.55	4.97		4.98	5.33	6.26
	1	3.94		4.14			[2]4.35		4.75		5.08	5.96
.1	0	3.93		4.09			[2]4.29		4.55		4.93	5.60
	1/3	3.75	3.82		4.02	4.02	4.09	4.39		4.42	4.70	5.33
	2/3	3.60	3.67		3.85	3.87	3.93	4.21		4.26	4.50	5.11
	1	3.46		3.62			[2]3.77		4.08		4.33	4.90
.2	0	3.09		3.18			[2]3.29		3.44		3.61	3.92
	1/2	2.92	2.97		3.06	3.08	3.12	3.25		3.31	3.43	3.75
	1	2.78		2.89			[2]2.98		3.15		3.28	3.60
.4	0	2.12		2.16					2.23		2.29	2.37
	1	1.98		2.01					2.11		2.18	2.27

(Sheet 1 of 3)

Table 1.--Buckling coefficients for simply supported panels (computer output) (continued)

S_x	t \ a/b	L_{cr}									
			m + n even			m + n odd			m + n even		
		0	.167	.250	.333	.333	.417	.542	.500	.542	.750	1.000
		$\alpha_1 = 1$, $\beta_1 = 1$, $\gamma_1 = .375$, $\alpha_2 = 1$, $\beta_2 = 0.6$, $\gamma_2 = 0.2$, $\theta = 2.5$										
0	0					(See $\theta = 1$)						
	1/3					(See $\theta = 1$)						
	2/3					(See $\theta = 1$)						
	1					(See $\theta = 1$)						
.05	0	4.33		4.50		[1]4.63			5.00		5.34	5.97
	1/3	4.14	4.21		4.40	4.42	4.49	4.77		4.84	5.09	5.68
	2/3	3.96	4.04		4.22	4.25	4.30	4.56		4.67	4.87	5.42
	1	3.81		3.97		[1]4.11			4.46		4.68	5.19
.1	0	3.61		3.70		[1]3.78			3.97		4.14	4.40
	1/2	3.41	3.47		3.54	3.58	3.61	3.71		3.81	3.92	4.17
	1	3.24		3.35		[1]3.42			3.61		3.76	3.97
.2	0	2.63		2.66		[1]2.67			2.71		2.78	2.84
	1	2.44		2.48		[1]2.49			2.54		2.63	2.68
.4	0	1.56		1.61					1.59		1.61	1.59
	1	1.52		1.55					1.54		1.57	1.55

(Sheet 2 of 3)

Table 1.--Buckling coefficients for simply supported panels (computer output) (continued)

S_x	t \ a/b	L_{cr}										
		m + n even				m + n odd			m + n even			
		0	.167	.250	.333	.333	.417	.542	.500	.542	.750	1.000
		$\alpha_1 = 1$, $\beta_1 = 1$, $\gamma_1 = .375$, $\alpha_2 = 1$, $\beta_2 = 0.6$, $\gamma_2 = 0.2$, $\theta = 0.4$										
0	0					(See $\theta = 1$)						
	1/3					(See $\theta = 1$)						
	2/3					(See $\theta = 1$)						
	1					(See $\theta = 1$)						
.05	0	4.62		4.85					5.59		6.26	(4)
	1/3	4.37	4.48		4.81	4.76	4.92	5.46		5.35	5.88	7.13
	2/3	4.17	4.28		4.57	4.55	4.67	5.17		5.11	5.56	6.73
	1	4.00		4.21					4.89		5.28	(4)
.1	0	4.08		4.27					4.86		5.39	(4)
	1/3	3.88	3.96		4.23	4.19	4.32	4.74		4.68	5.10	6.09
	2/3	3.71	3.79		4.04	4.02	4.12	4.52		4.49	4.85	5.80
	1	3.56		3.74					4.30		4.65	(4)
.2	0	3.32		3.46					3.87		4.22	(4)
	1/2	3.10	3.17		3.35	3.34	3.41	3.70		3.68	3.96	4.63
	1	2.93		3.07			[2]3.22		3.48		3.74	(4)
.4	0	2.42		2.51					2.74		2.94	(4)
	1	2.19		2.28					2.52		2.69	(4)

[1] a/b = .330

[2] a/b = .410

[3] a/b = .170

[4] Use values from $\theta = 2.5$ to construct a curve.

(Sheet 3 of 3)

Table 2. --Buckling coefficients for simply supported panels (computer output)

θ	S_x \ a/b	L_{cr}								
			m + n even		m + n odd			m + n even		
		0	.167	.333	.333	.417	.542	.542	.750	1.000
		$\alpha = 1.5,\ \beta = 0.6,\ \gamma = 0.2$								
0.4	0	(See $\theta = 1$ in table 1)								
	.1	3.97	4.04	4.18	4.25	4.32	4.47	4.68	4.91	5.40
	.4	2.22	2.25	2.31	2.34	2.37	2.45	2.52	2.63	2.91
1	0	5.61	5.73	5.93	6.05	6.15	6.41	6.77	7.12	7.90
	.1	3.87	3.92	4.04	4.08	4.17	4.26	4.44	4.64	4.96
	.4	2.01	2.03	2.06	2.06	2.09	2.10	2.14	2.20	2.27
2.5	0	(See $\theta = 1$ in table 1)								
	.1	3.62	3.67	3.74	3.73	3.82	3.86	3.93	4.12	4.22
	.4	1.56	1.64	1.58	1.60	1.57	1.60	1.58	1.61	1.58
		$\alpha = .667,\ \beta = 0.6,\ \gamma = 0.2$								
.4	0	(See $\theta = 1$ in table 1)								
	.1	3.11	3.24	3.60	3.44	3.67	4.29	3.91	4.50	5.89
	.4	2.10	2.16	2.32	2.26	2.35	2.60	2.50	2.74	3.25
1	0	3.74	3.91	4.41	4.18	4.53	5.44	4.83	5.72	7.90
	.1	3.03	3.13	3.41	3.30	3.46	3.90	3.68	4.06	4.96
	.4	1.89	1.92	1.96	1.97	1.99	2.06	2.07	2.12	2.27
2.5	0	(See $\theta = 1$ in table 1)								
	.1	2.84	2.89	3.03	3.01	3.06	3.27	3.27	3.40	3.77
	.4	1.46	1.48	1.48	1.48	1.48	1.48	1.49	1.50	1.50

Table 3.--Results of tests of square, flat panels of symmetrical, isotropic sandwich constructions in shear

Specimen No.	Thicknesses: Facing[1] f	Thicknesses: Core c	Thicknesses: Total	Panel size a	Buckling load P	Maximum load	Facing stress at buckling load q'_f	Core shear modulus μ_c	S[2]	L_{cr}[2]	Computed[3] buckling stress q_f
	In.	In.	In.	In.	Lb.	Lb.	P.s.i.	P.s.i.			P.s.i.
					CORES OF CORKBOARD						
16	0.020	0.142	0.182	16	6,500	6,700	7,180	1,500	0.400	2.57	.....
17	.032	.148	.212	16	11,800	12,300	8,140	1,500	.669	2.35	.....
18	.020	.139	.179	16	5,200	5,540	5,740	950	.620	2.13	.....
13	.020	.132	.172	18	3,200	3,700	3,140	320	1.382	1.61	.....
14	.032	.133	.197	14	5,800	7,550	4,570	320	3.680	1.20	.....
15	.012	.118	.142	18	2,000	2,140	3,270	320	.741	2.31	.....
					CORES OF HARD SPONGE RUBBER						
61	.032	.137	.201	14	14,600	14,600	11,500	3,400	.356	2.88	.....
62	.032	.129	.193	14	14,100	14,100	11,100	3,400	.336	3.06	.....
71	.032	.133	.197	18	15,700	15,700	9,600	3,400	.210	4.16	.....
72	.032	.134	.198	18	14,950	14,950	9,200	3,400	.211	3.94	.....
81	.032	.137	.201	21	17,750	17,750	9,300	3,400	.159	5.23	.....
82	.032	.139	.203	21	17,500	17,500	9,200	3,400	.161	5.06	.....
83	.032	.152	.216	21	15,200	15,200	8,000	3,400	.176	3.80	.....
91	.032	.127	.191	26	16,000	17,150	6,800	3,400	.096	6.62	.....
92	.032	.132	.196	26	18,000	23,550	7,600	3,400	.100	6.96	.....
93	.032	.127	.191	26	17,000	17,550	7,200	3,400	.096	7.01	.....
101	.032	.126	.190	34	16,000	17,440	5,200	3,400	.056	8.76	.....
102	.032	.123	.187	34	20,000	20,000	6,500	3,400	.054	11.37	.....
					CORES OF END-GRAIN BALSA						
1	.012	.125	.149	20	10,000	11,150	14,700	15,000	.013	11.48	.....
3	.012	.126	.150	20	5,200	5,200	7,660	15,000	.013	5.90	.....
4	.012	.127	.151	20	8,790	8,790	12,940	15,000	.013	9.82	.....
5	.012	.127	.151	20	5,360	5,360	7,890	15,000	.013	5.98	.....
20	.012	.125	.149	20	6,700	6,700	9,870	15,000	.013	7.73	.....
19	.020	.124	.164	20	16,080	16,080	14,200	15,000	.023	10.05	.....
121	.020	.243	.283	20	34,000	36,150	30,000	15,000	.....	.....	29,600
122	.020	.242	.282	17	30,650	30,650	31,900	15,000	.....	.....	31,700

[1]All facings were sheets of clad 24S-T3 aluminum alloy, E_f = 10,000,000 p.s.i.

[2]$S = \dfrac{\pi^2 c f E_f}{2 \lambda_f a^2 \mu_c}$ $\quad L_{cr} = \dfrac{4 \lambda_f a^2}{\pi^2 h^2 E_f} q'_f$

[3]Values in this column were computed for stresses above the proportional limit for which values of S could not be computed. The edges were assumed to be simply supported.

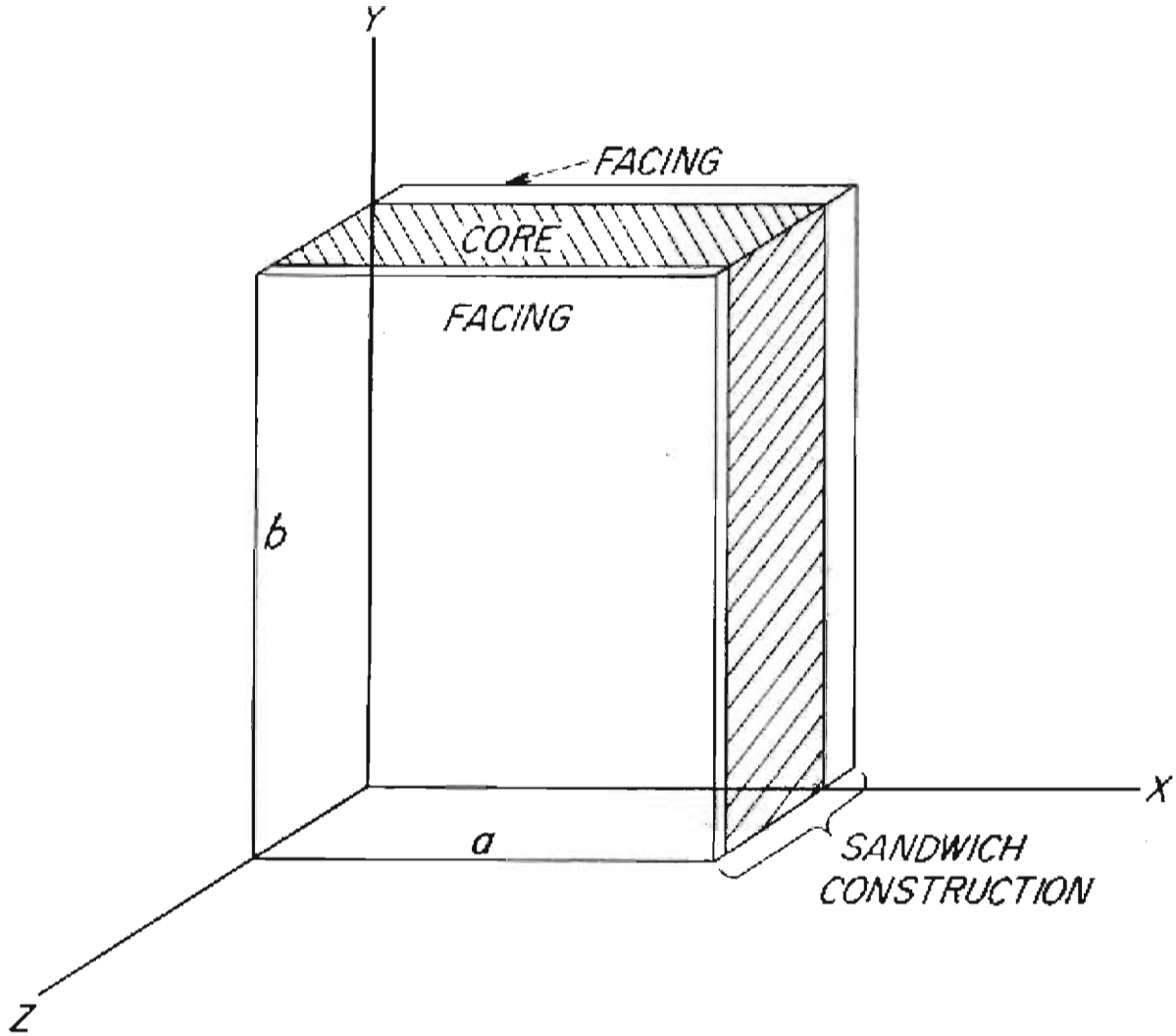

Figure 1. --Sketch showing position of axes relative to the sandwich construction.

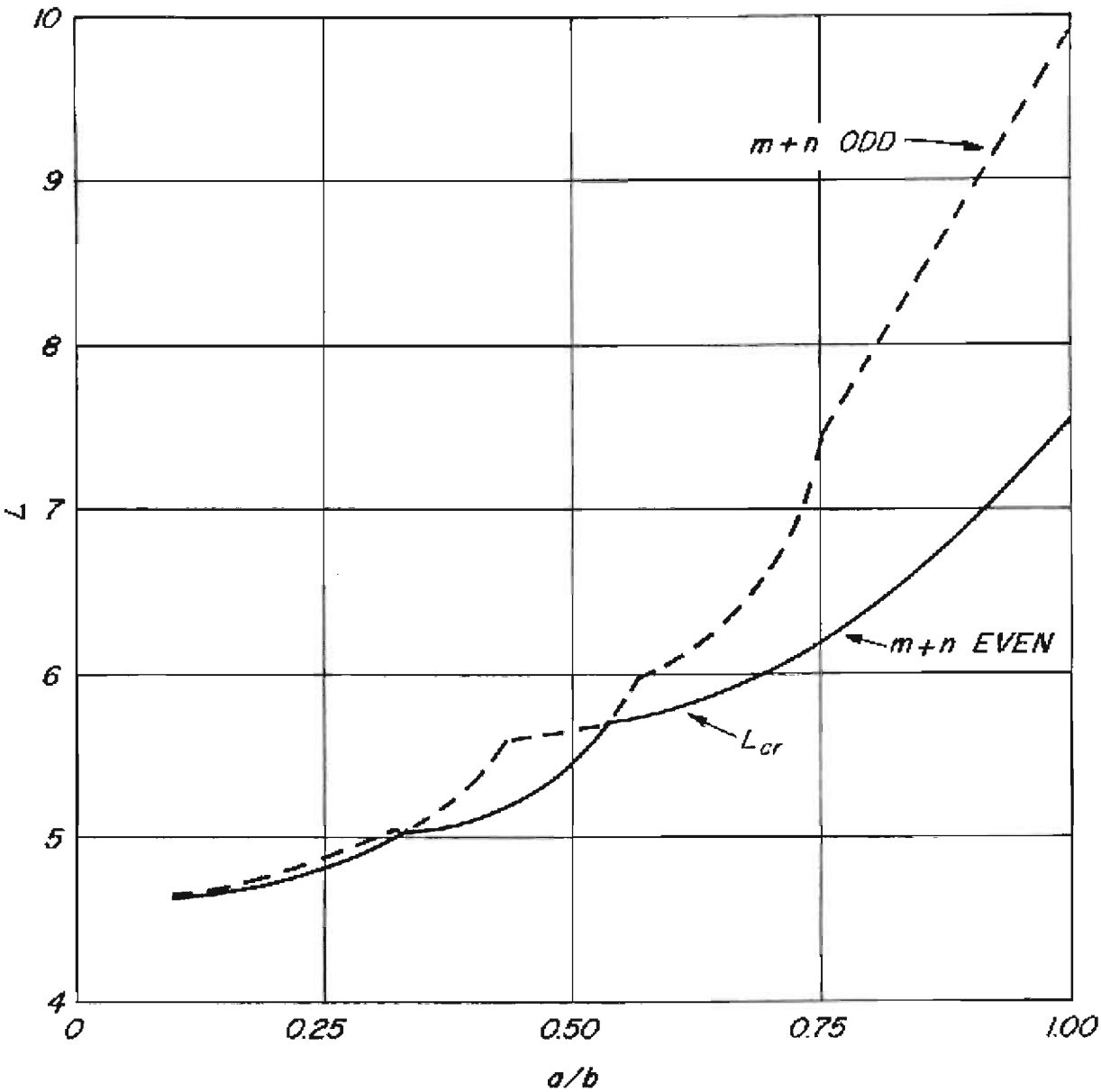

Figure 2.--Both roots of determinant of system (9). At any $\frac{a}{b}$, lower root is L_{cr}.

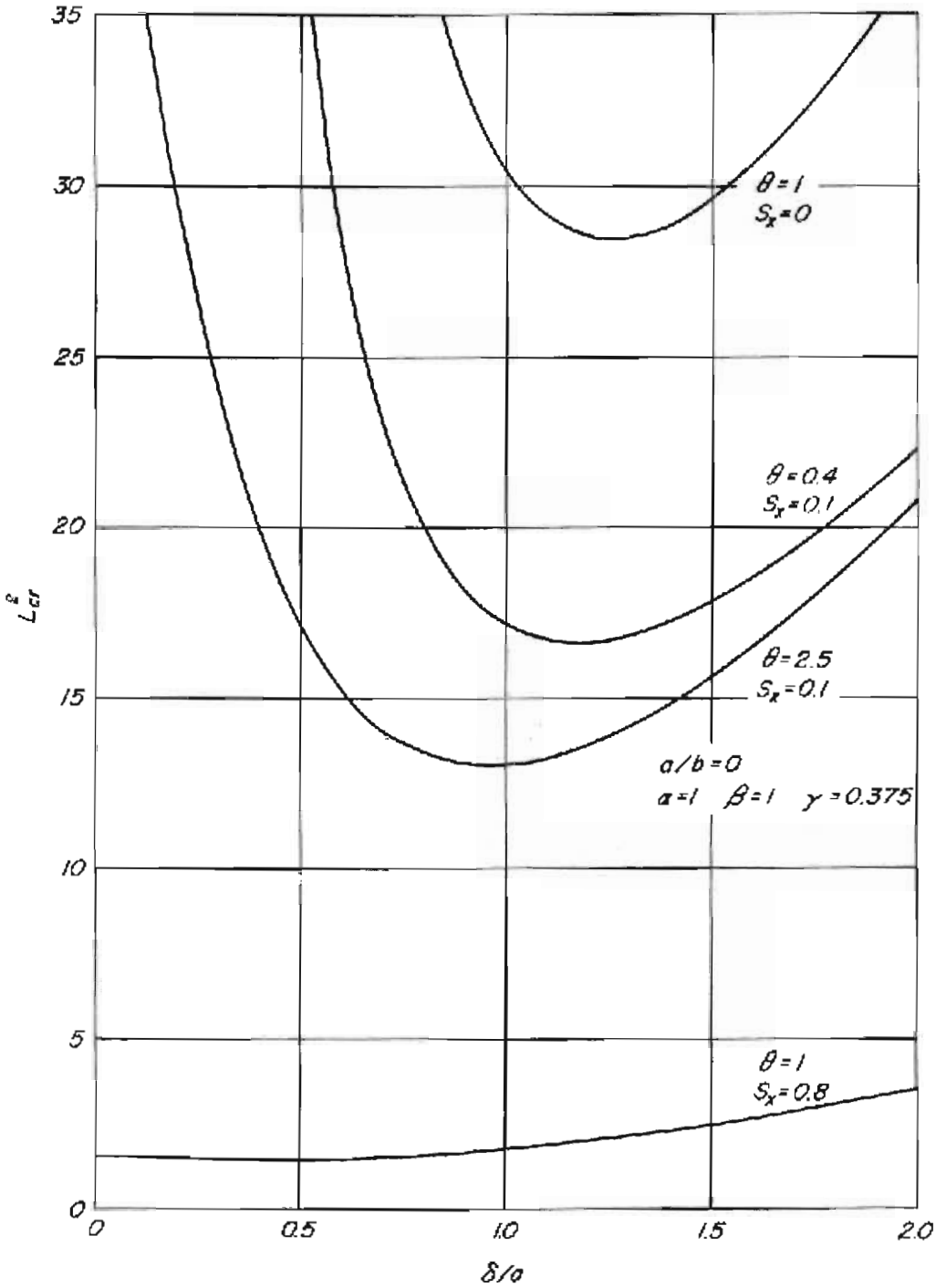

Figure 3.--Effect of buckle size on critical load of infinite long panels.

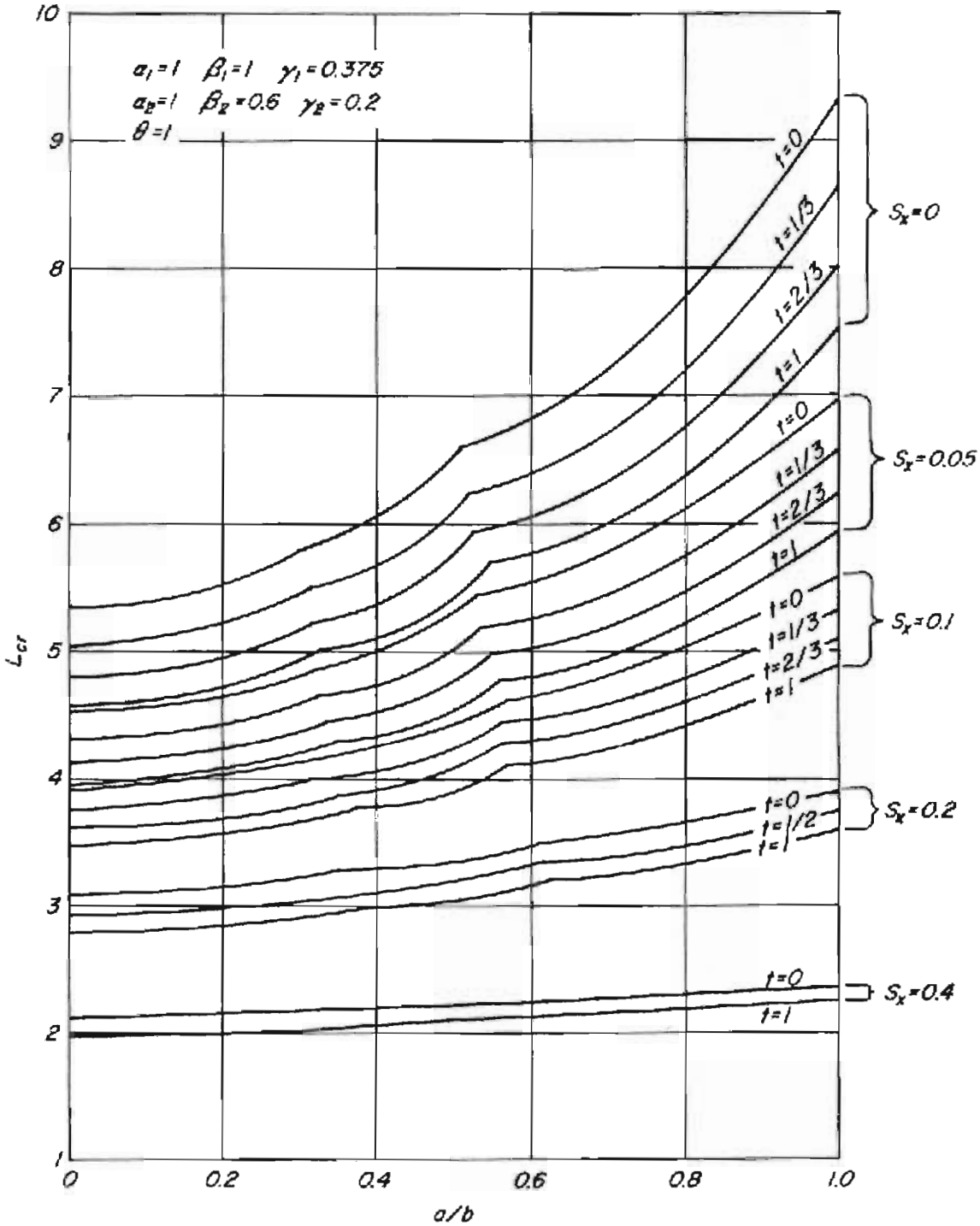

Figure 4.--Buckling coefficient, L_{cr}, for simply supported sandwich panels with isotropic core in edgewise shear.

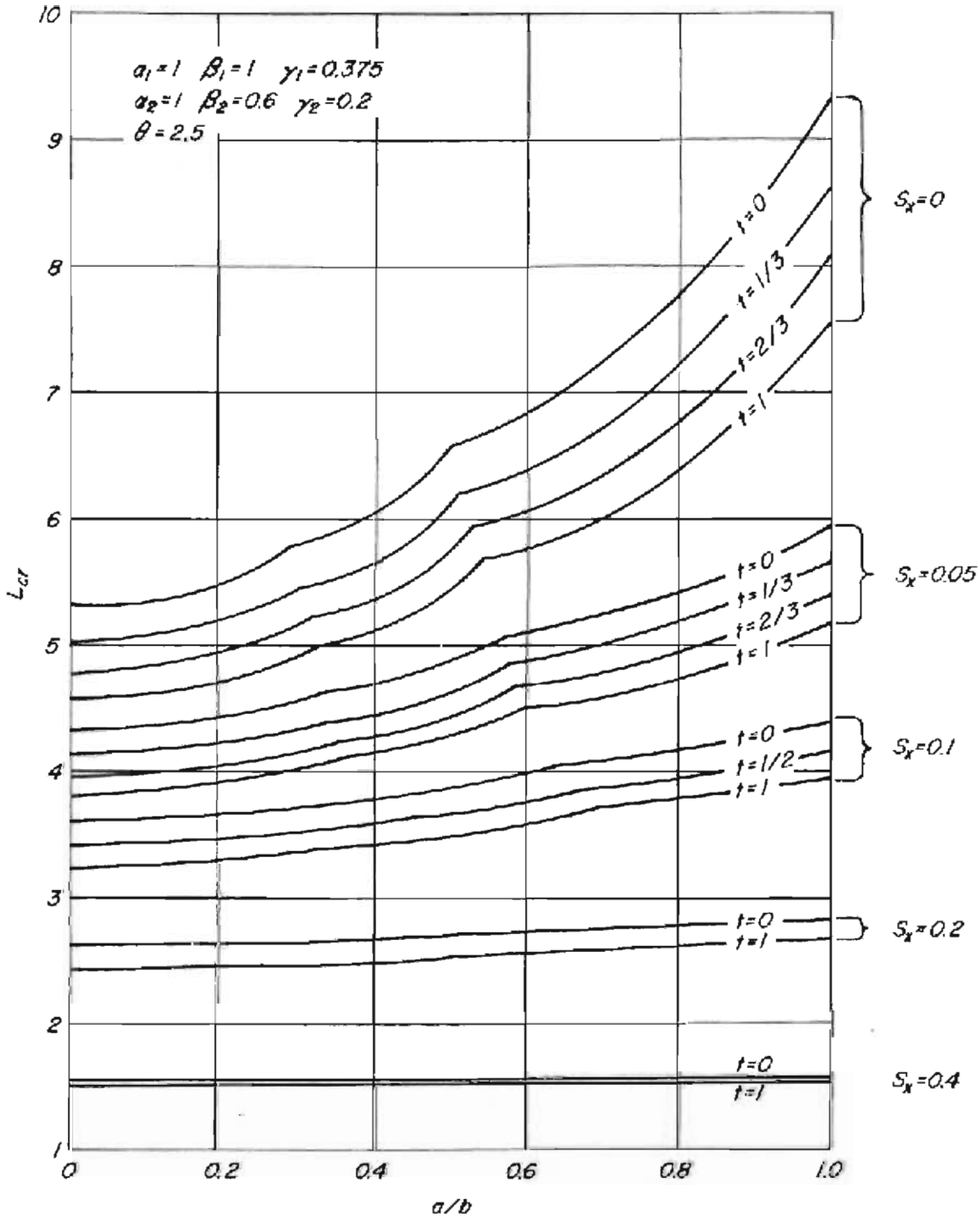

Figure 5.--Buckling coefficient, L_{cr}, for simply supported sandwich panels with orthotropic core in edgewise shear.

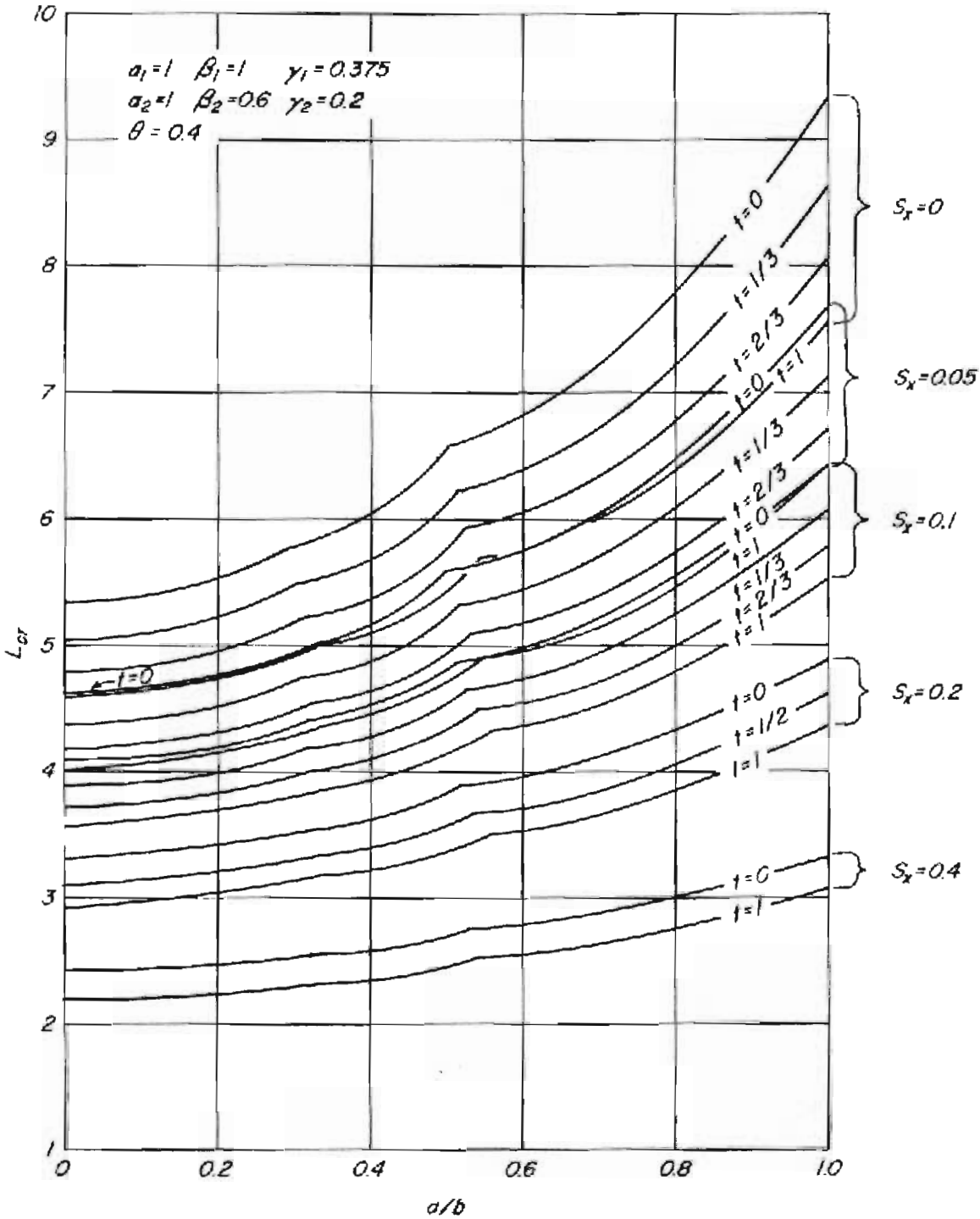

Figure 6.--Buckling coefficient, L_{cr}, for simply supported sandwich panels with orthotropic core in edgewise shear.

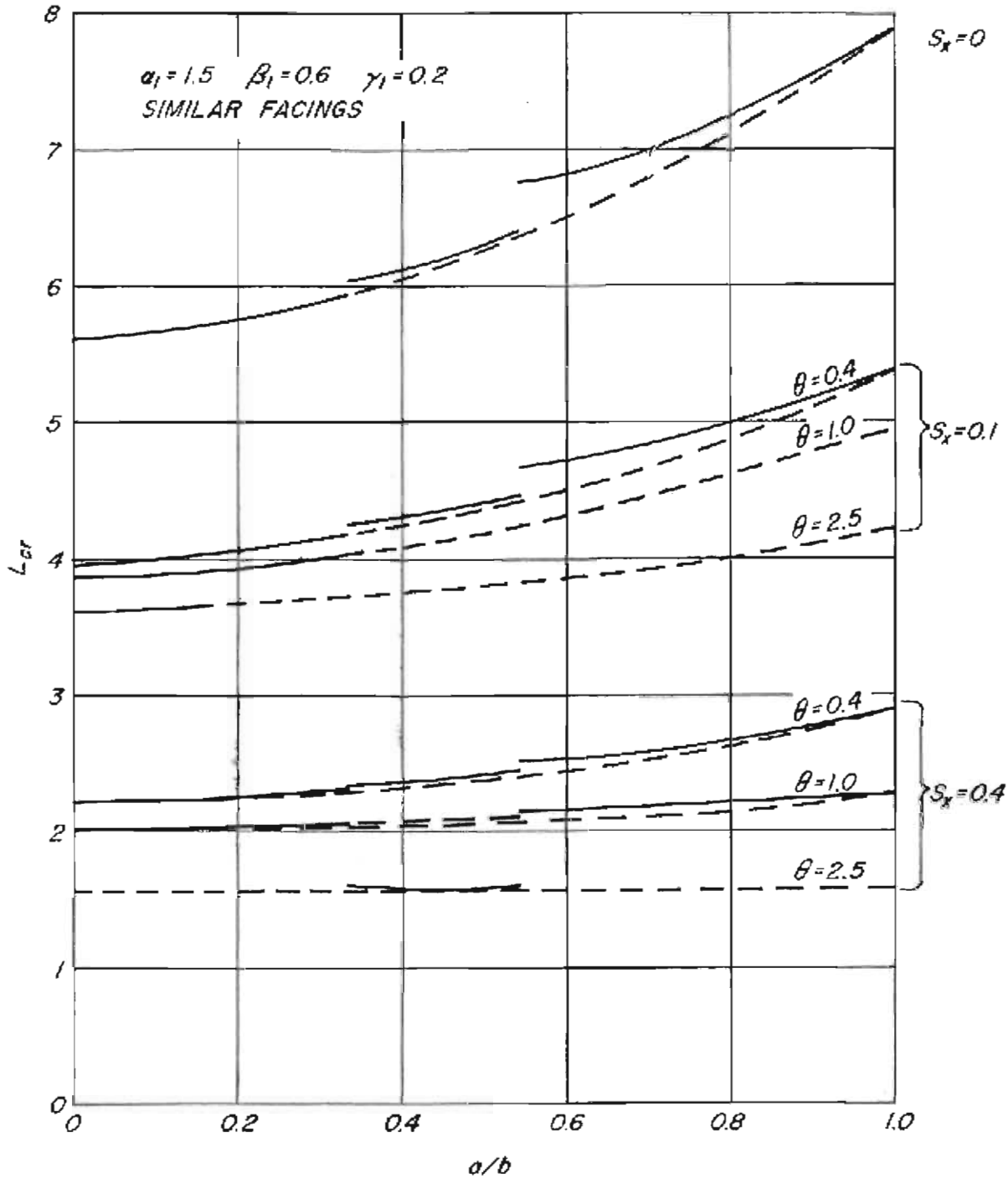

Figure 7.--Buckling coefficient, L_{cr}, for simply supported sandwich panels with orthotropic facings in edgewise shear.

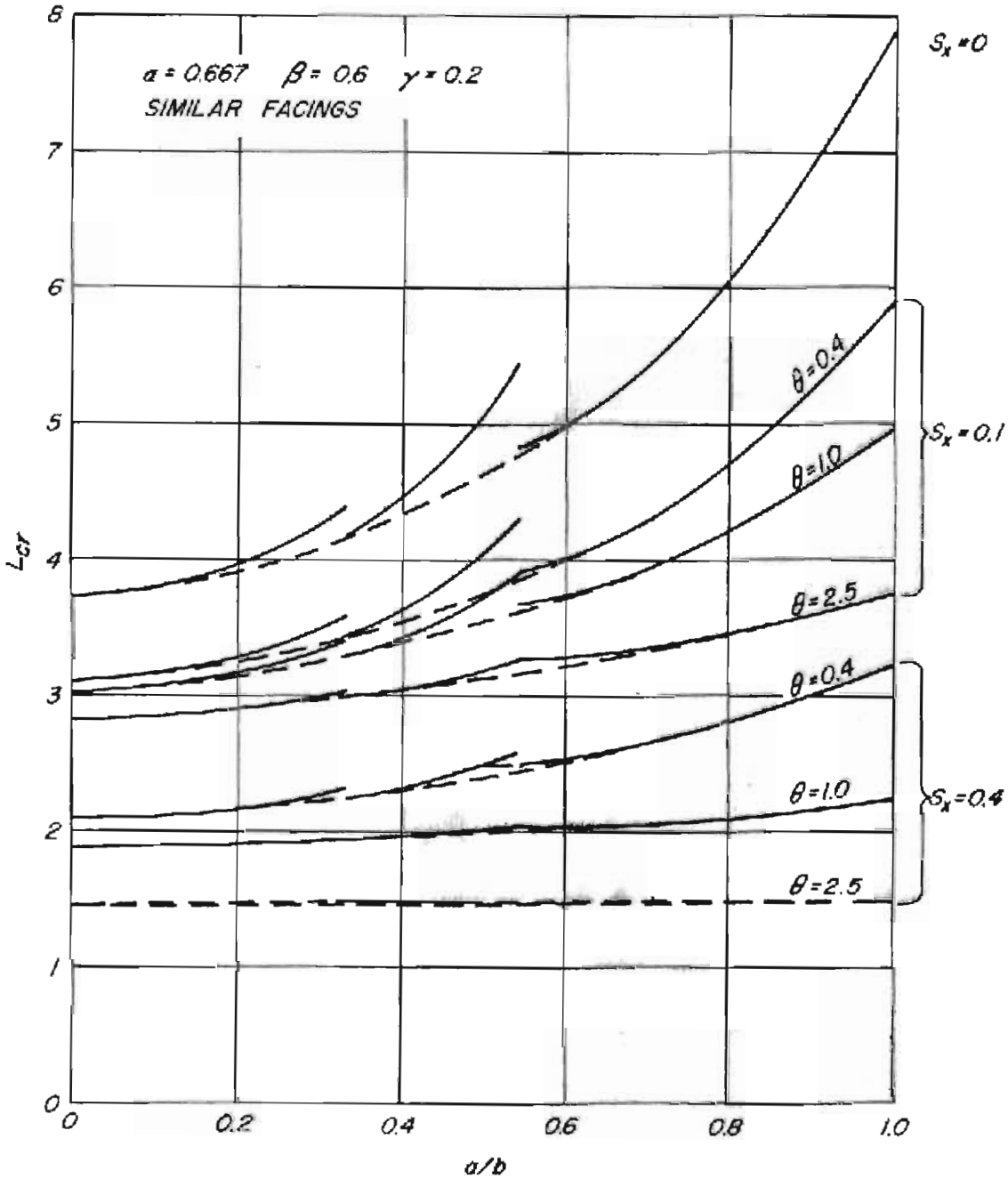

Figure 8.--Buckling coefficient, L_{cr}, for simply supported sandwich panels with orthotropic facings in edgewise shear.

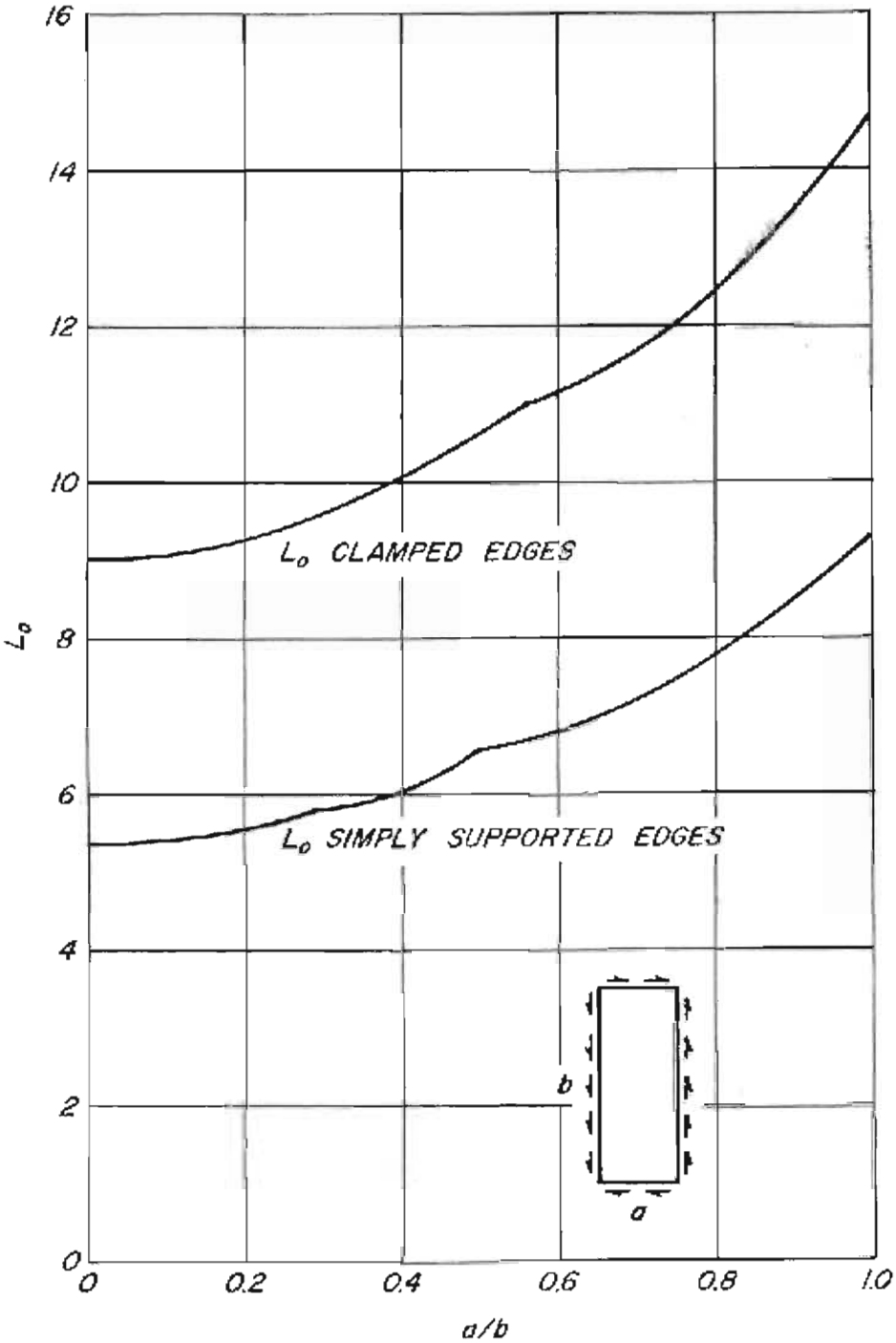

Figure 9. --Buckling load factor of homogeneous isotropic plates. Upper curve from reference (9).

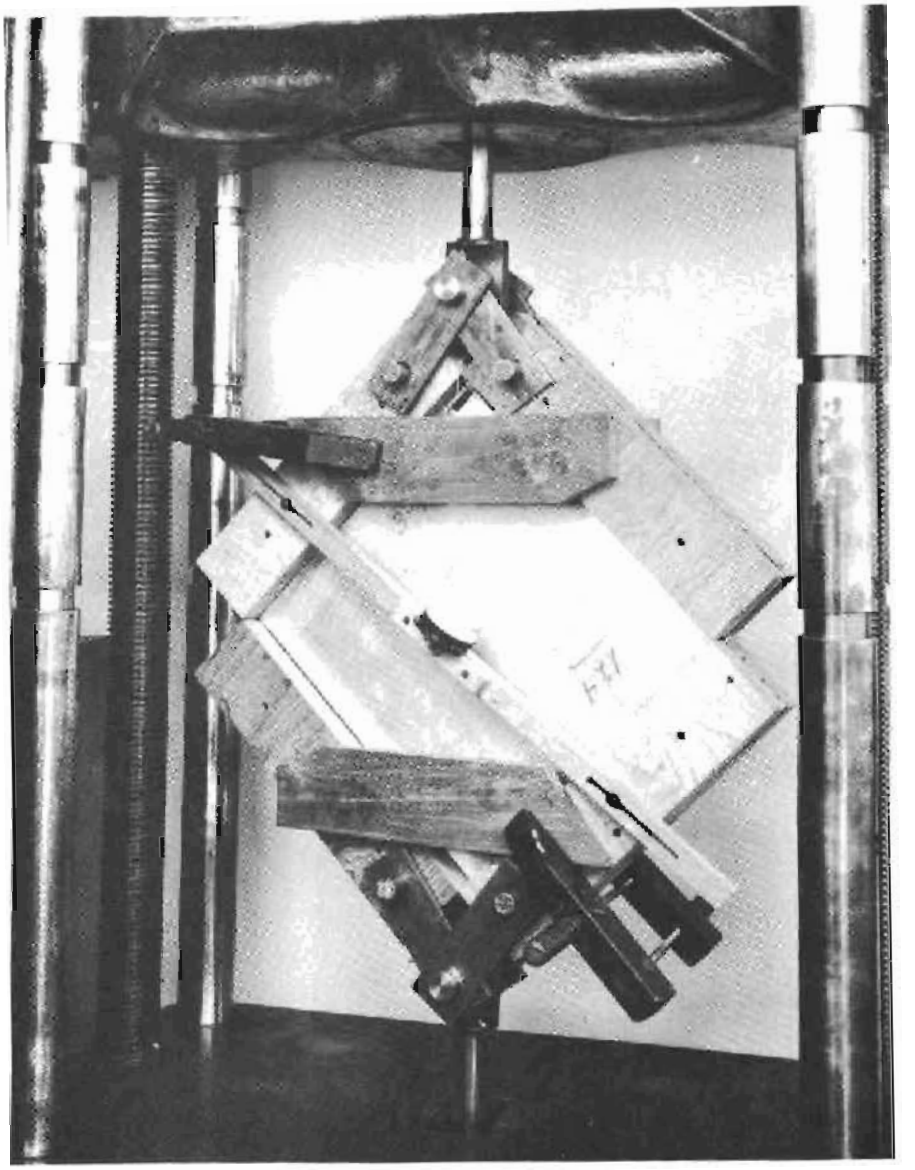

Figure 10.--Arrangement of apparatus for testing a square, flat panel of sandwich construction in shear.

Z M 84365 F

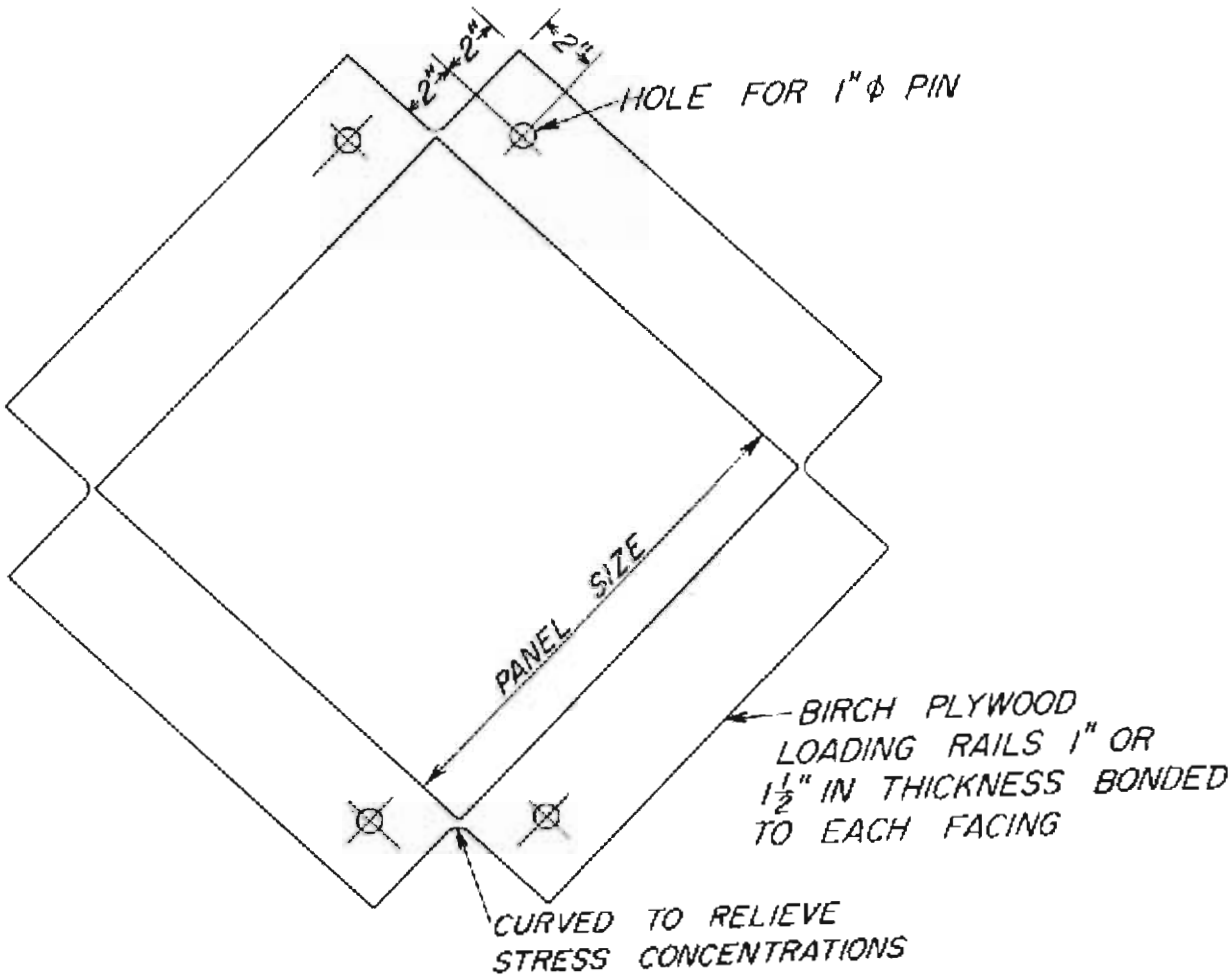

Figure 11.--Sketch showing arrangement of loading rails and pin positions for testing square, flat sandwich panels in shear.

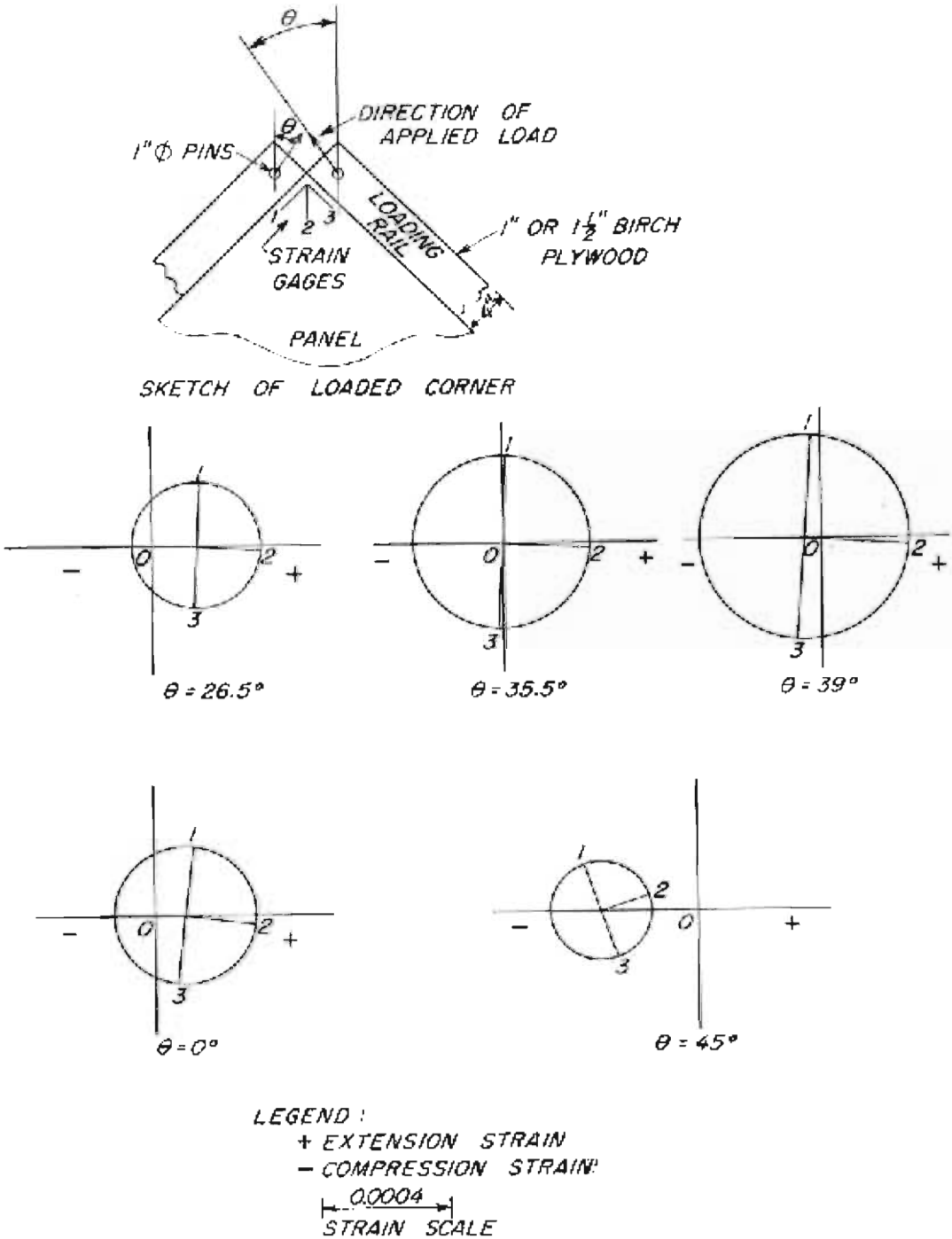

Figure 12. --Strain circles of strains measured in loaded corner showing variation in quality of shear as direction of applied load was changed. Data from panel 121 at P = 5,000 pounds.

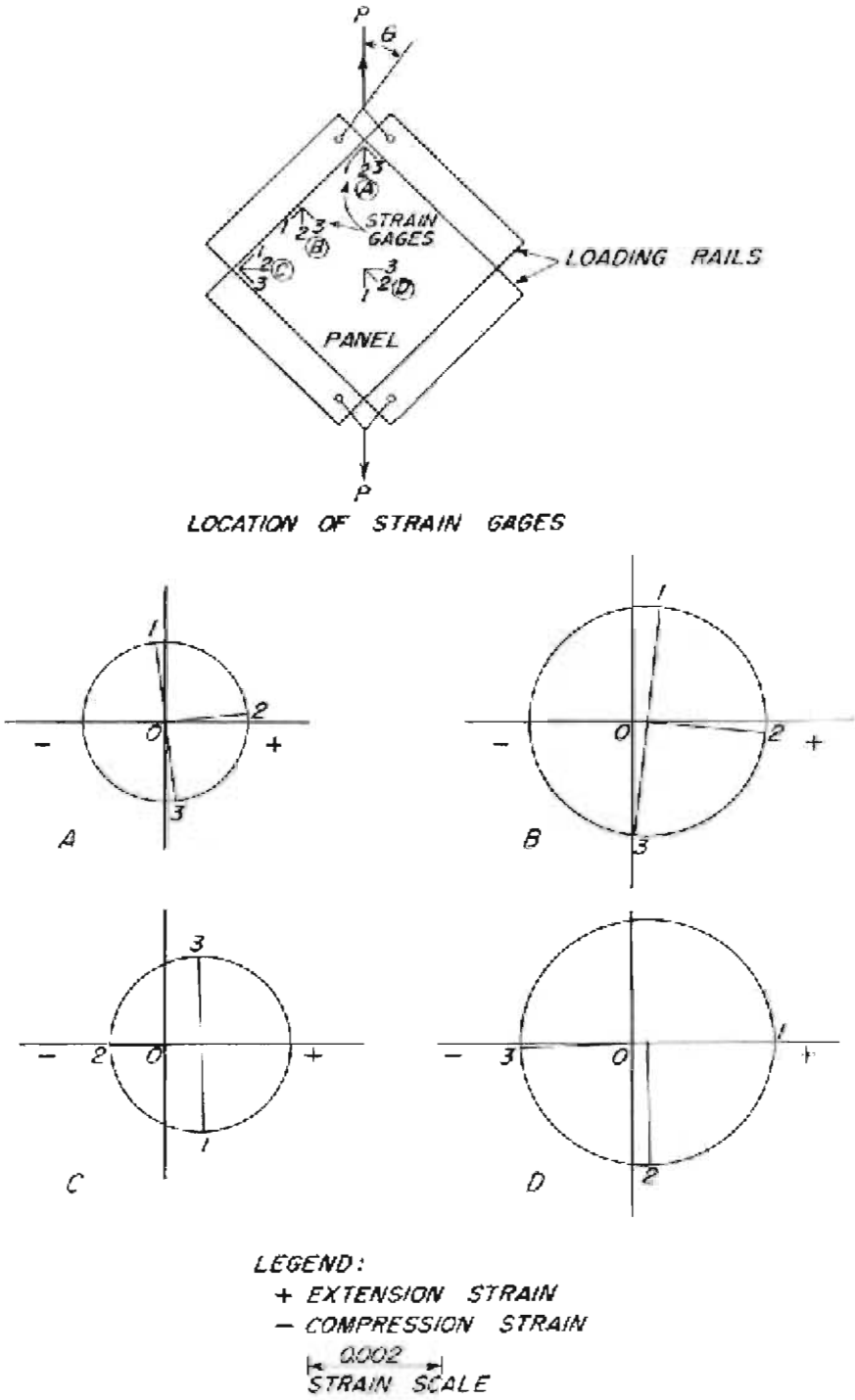

Figure 13.--Strain circles of strains measured at various locations on panel 12k at P = 20,000 pounds at θ = 35.5°.

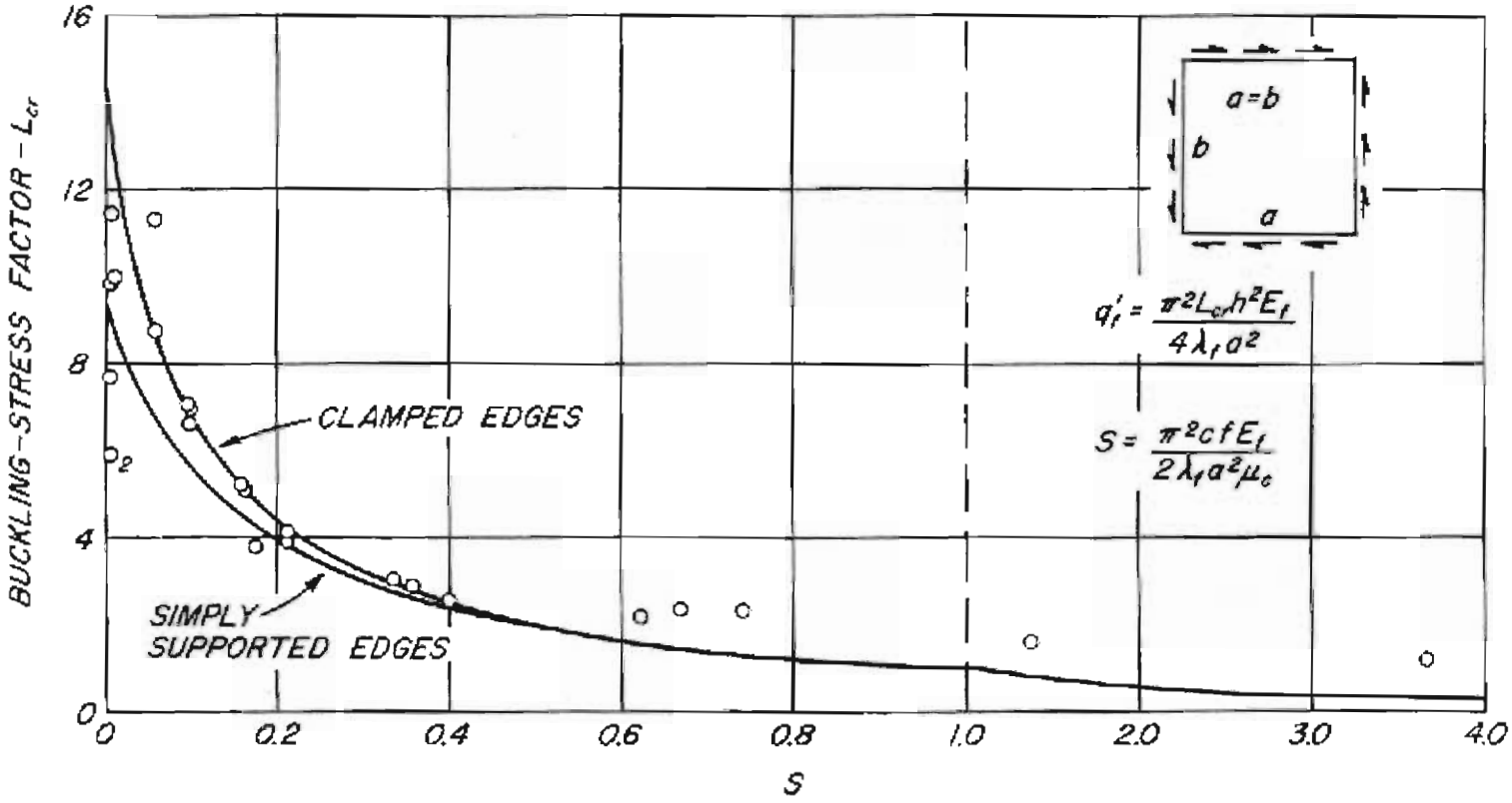

Figure 14.--Comparison of experimental buckling-stress factors with theoretical curves of factors for square, flat panels of symmetrical, isotropic sandiwch constructions in shear. (Note change of abscissa scale at S = 1.0.)

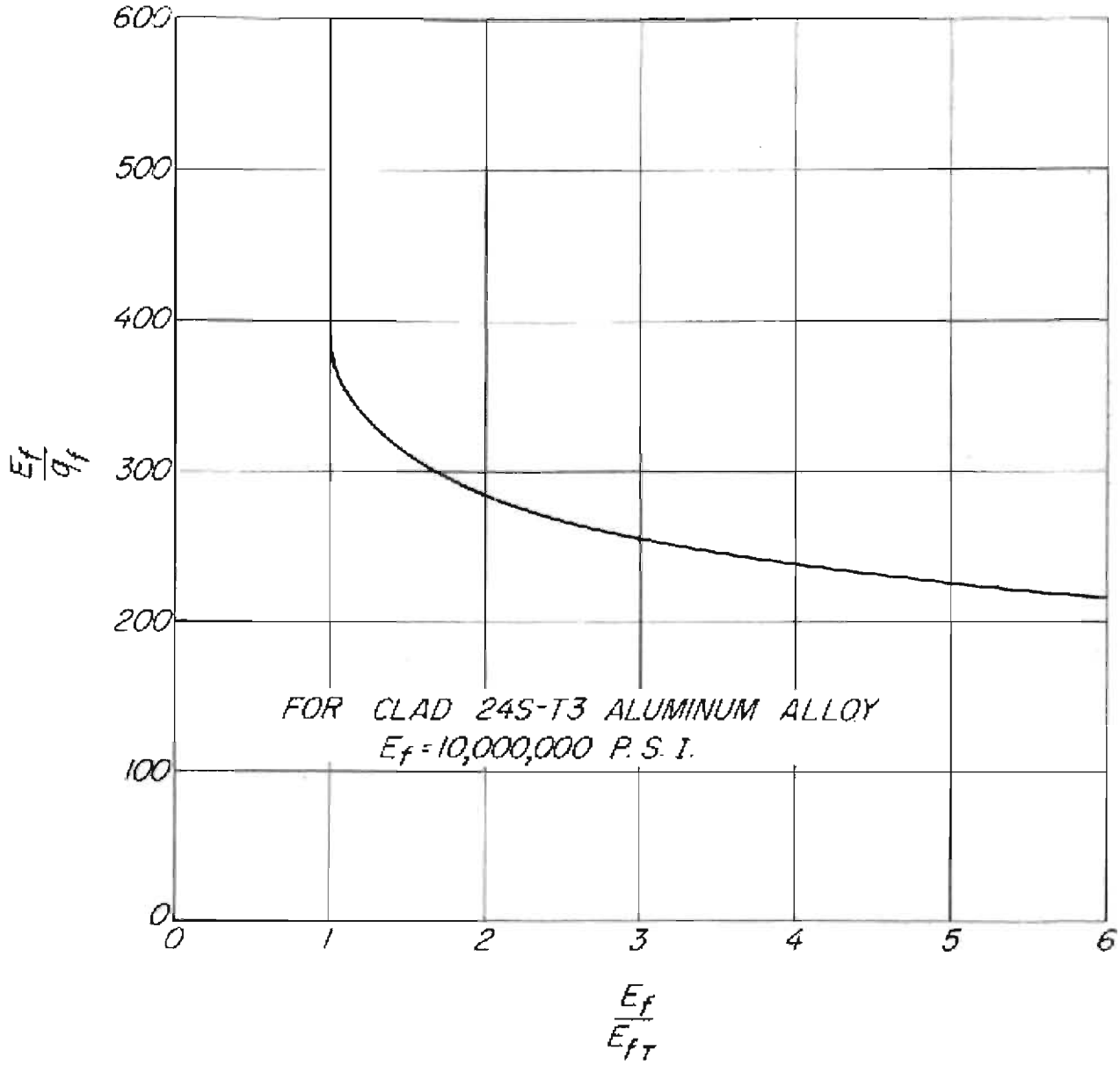

Figure 15.--Reciprocal stress-modulus curve of clad 24S-T3 aluminum alloy for use at stresses above proportional limit values.

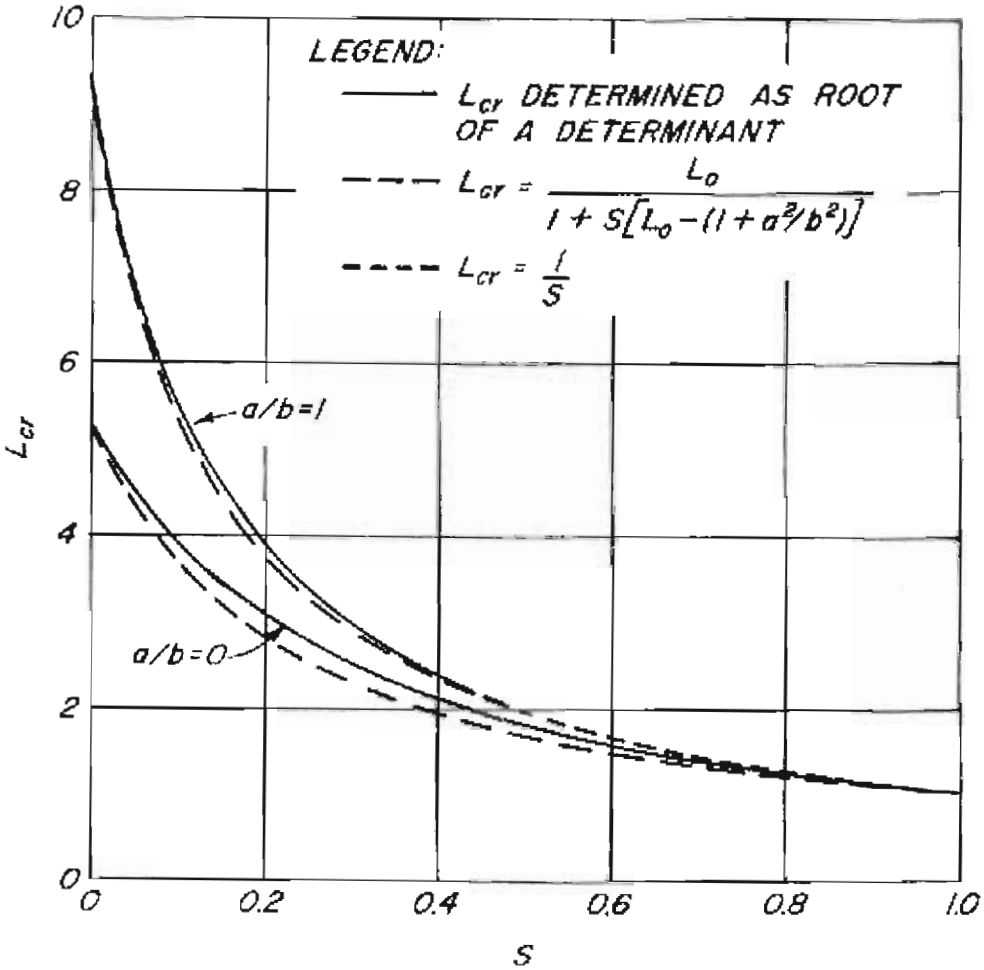

Figure 16.--Comparison of exact and approximate solutions for isotropic panels.

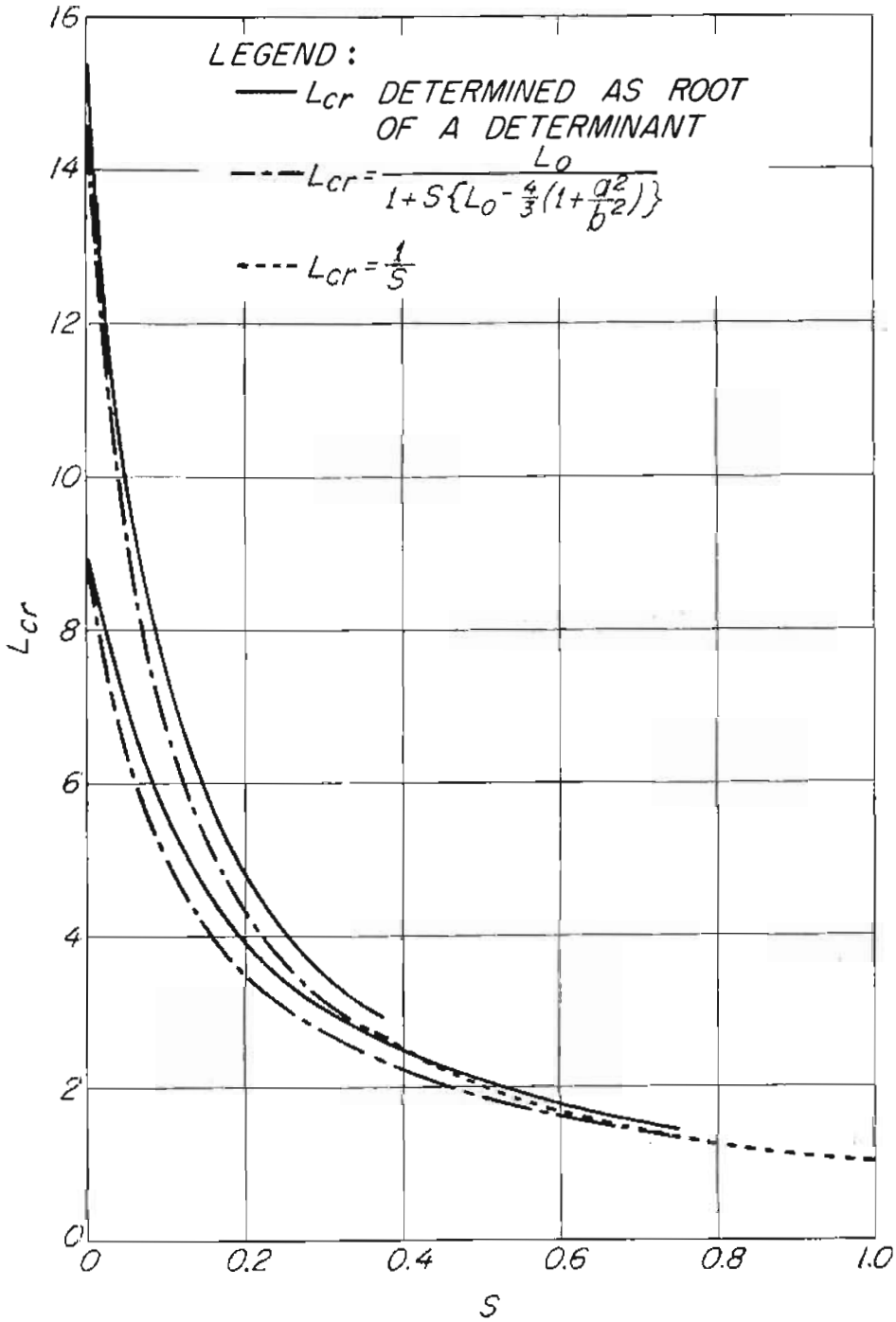

Figure 17.--Buckling load factors for clamped panels. Results by computations and approximating curves for $\frac{a}{b} = 1$ and $\frac{a}{b} = 0$.